



Spatial analysis and site formation processes associated with the Middle Pleistocene hominid teeth from Q1/B waterhole, Boxgrove (West Sussex, UK)

Laura Sánchez-Romero^{1,2} · Alfonso Benito-Calvo³ · Dimitri De Loecker⁴ · Matthew Pope⁵

Received: 9 February 2023 / Accepted: 12 May 2023 / Published online: 13 June 2023
© The Author(s) 2023

Abstract

Boxgrove is a key locale for our understanding of Middle Pleistocene human behaviour in Northwestern Europe. It provides high-resolution evidence for behaviour at scale in fine-grained sediments, dating from the end of the MIS13 interglacial at around 480,000 years ago. Excavations at this site in the last quarter of the twentieth century have provided a large body of interdisciplinary data, comprising stone artefact assemblages, well-preserved faunal remains and paleoenvironmental archives, from over 100 test pits and larger excavation areas. The excavation area designated Q1/B was excavated between 1995 and 1996 and provided a particularly deep and complex record of early human activity centred upon a pond or waterhole within the wider landscape. In this work, we present a new analysis of spatial data from a single sedimentary unit (Unit 4u) at the Boxgrove Q1/B site. We consider the spatial disposition of lithic and faunal materials, fabric analysis and the role of the palaeotopography in their distribution. The results indicate that, although the dynamic fluvial depositional environment had an undeniable role in the distribution of materials, the scale and nature of post-depositional movement are consistent with the artefacts being preserved within an autochthonous depositional context, not reworked from an earlier sedimentary unit or subject to long-distance transportation. These results are consistent with previous analysis which suggests that the overall lithic assemblage can be directly compared with others from the wider landscape in compositional terms to interpret the behavioural controls over site formation behind the Q1/B archaeology.

Keywords Formation processes · Palaeotopographic reconstruction · Spatial analysis · GIS · Open-air site · Middle Pleistocene

Introduction

Site formation processes are one of the most important subjects investigated in Palaeolithic archaeology and have gained more importance in the last few years thanks to the advances in research, new analysis techniques and ease of access to GIS tools. These factors, together with the growing interest in understanding how the site was formed and who was responsible for the accumulation of materials, beyond directly attributing this responsibility to humans, have produced a proliferation of spatial studies. Spatial analysis in the archaeological record of open-air sites has traditionally been more considered because the environment is usually more favourable, since the rapid sedimentation and, therefore, the materials are buried more quickly. This means they are not exposed for a long time and are protected from post-depositional processes. The lacustrine and palustrine environments allow this preservation, since

✉ Laura Sánchez-Romero
lausanrom@gmail.com

¹ Centre d'Estudis del Patrimoni Arqueològic, Universitat Autònoma de Barcelona, 08193 Bellaterra, Spain

² Human Evolution Research Center, University of California, 3101 Valley Life Sciences Building, Berkeley, CA 94720, USA

³ Centro Nacional de Investigación sobre la Evolución Humana, P Sierra de Atapuerca, 3, 09002 Burgos, Spain

⁴ Faculty of Archaeology (Human Origins), Leiden University, Einsteinweg 2, 2333 CC Leiden, The Netherlands

⁵ UCL Institute of Archaeology, University College London, 31-34 Gordon Square, London WC1H 0PY, UK

the dynamics characterized by a low-very-low deposition of sediments burying the archaeological assemblages, allowing their good preservation (Behrensmeier 1988; Conard et al. 2015).

In this work, we present the spatial study of the open-air site of Q1/B, one of the Boxgrove localities. This Middle Pleistocene site can be compared with other open-air sites of similar chronology, such as Schöningen, Neumark-Nord 1 and Kärliche-Seeufer in Germany (Mania 1990, 2004; Gaudzinski et al. 1996; Thieme 1997; Fisher 2010; Böhner et al. 2015; Serangeli et al. 2015; Hutson et al. 2020; García-Moreno et al. 2021), Ambrona in Spain (Pérez-González et al. 2005; Falguères et al. 2006; Sánchez-Romero et al. 2016), Castel di Guido and La Polledrara di Cecanibbio in Italy (Radmilli and Boschian 1996; Boschian and Saccà, 2010, 2015; Anzidei et al. 2012; Santucci et al. 2016) or Gesher Benot Ya'aqov (slightly older) and Revadim Quarry in Israel (Goren-Inbar et al. 1994; Alperson-Afil et al. 2009; Marder et al. 2010; Malinsky-Buller et al. 2011), among many others. All of these sites demonstrate how important it is to make detailed studies that consider all of the aspects within an archaeological site, from stratigraphy to taphonomic studies of bones, analysis of lithic industry and bones, micromorphology or even the estimation of organic layers as in the case of Schöningen (Böhner et al. 2015). All disciplines provide very useful data that converge in spatial studies to work out what happened and what role the biotic and abiotic factors played in the formation of the site.

This work addresses the site formation processes from the perspective of the information provided by the excavated materials, together with the data provided by previous stratigraphic studies. Through all this information brought together, we intend to understand the role that anthropological and natural factors may have played in the preservation of the deposit, as far as the distribution of materials, so the affectation degree of such processes can be evaluated and, at the same time, to understand the role of the human groups responsible for the presence of archaeological materials in the site. Therefore, the distribution patterns, clusters and fabrics of the archaeo-paleontological materials have been analysed, and they have been cross-referenced with the characteristics of the sedimentary deposit. Additionally, we will consider the impact of the natural factors inherent in any site, even more so in open-air sites, on the preservation of the materials. With this, we intend to address the history of the site itself and isolate those key elements that participated in the formation of the site, with the aim to learn more about the mobility patterns, functionality and intra-site dynamics of the past human groups that visited Boxgrove.

Boxgrove site complex

The Boxgrove site complex (West Sussex, UK) is situated 50 m above sea level and about 10 km from the present-day coastline of the English Channel (Fig. 1). The quarries at Boxgrove were first dug during the Second World War (Pope et al. 2020), but its archaeological importance was not recognized until 1974, during sand and gravel extraction in a quarry called Amey's Eartham Pit. During its discovery, particularly between 1982 and 1996, when excavation was directed by Mark Roberts and Simon Parfitt of the University College of London (UCL) Institute of Archaeology, over 100 individual localities were excavated, and a high-resolution record of lithic artefacts and fossilized mammal remains was recovered from a succession of buried land surfaces (Roberts et al. 1986; Roberts and Parfitt 1999).

Most of the high-resolution archaeological record comes from fine-grained intertidal and paleosol sediments, attributed to the cold substages of the MIS13 interglacial at about 480 ka (Preece and Parfitt 2012; Whittaker and Parfitt 2017). This record has been mapped across 26 km and includes locales such as Slindon and the Valdoe, as well as the main Boxgrove site (Pope 2001; Pope et al. 2009; Roberts and Pope 2009, 2018). The overlying cold-stage deposits have been correlated with the major glacial period of MIS12 (Preece and Parfitt 2012). The warm-stage interglacial deposits at the base of the Boxgrove sequence have been dated primarily on the basis of mammalian biostratigraphy (Roberts and Parfitt 1999). There is a combination of large and small mammals that went extinct at the end of the early Middle Pleistocene (Roberts and Parfitt 1999), comprising *Stephanorhinus hundesheimensis*, *Megaloceros verticornis*, *M. savini*, *M. dawkinsi*, *Ursus deningeri* and *Pliomys episcopalpis* (Roberts and Parfitt 1999). In addition, there are early forms of the living water vole (*Arvicola*) and narrowed-skulled vole (*Microtus gregalis*) that together characterize the latter part of the "Cromerian Complex" correlated with MIS13.

In this work, we focus on one of the localities excavated in Boxgrove, the Q1/B site. This open-air site has provided many well-preserved lithic materials and bones, as well as an incomplete tibia and two lower front incisors broadly ascribed to *Homo heidelbergensis* (Roberts et al. 1994; Stringer et al. 1998; Hillson et al. 2010). While previous publications have considered aspects of the bifacial technology from the site (Stout et al. 2014; García-Medrano et al. 2019), as well as environmental context and overview of site formation processes (Pope 2002; Preece and Parfitt 2012; Whittaker and Parfitt 2017), this is the first detailed, standalone study focused exclusively on Q1/B

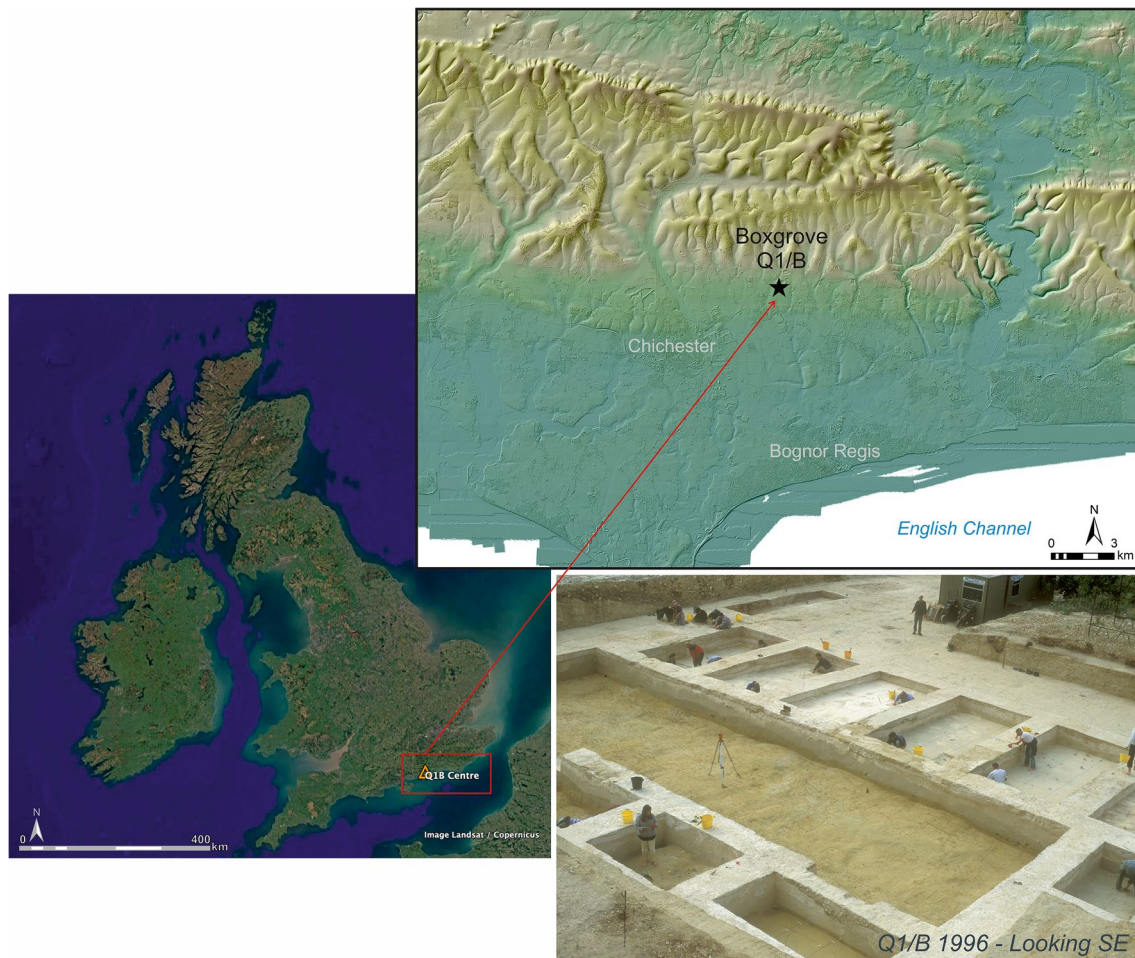


Fig. 1 Location of the Pleistocene site of Boxgrove Q1/B in West Sussex, UK. Source of the LiDAR maps: UK Centre For Ecology & Hydrology Licence Agreement. Environment Agency. Open Government Licence v3.0

that considers the formation of the site, distinguishing the role played by humans in the composition and spatial arrangement of lithic and bone assemblage from one of its depositional units. The spatial analysis presented here aims to know the formation dynamics and occupation patterns of the site, to shed more light on the settlement models of these human groups.

The Boxgrove Q1/B site

The Q1/B excavation area is situated in the northwest corner of Quarry 1, the western-most of the quarries at Amey's Eartham Pit. While excavation was started in this area in the late 1980s, it was not until 1993 and the discovery of a human tibia associated with well-preserved mammal fauna and a stone artefact assemblage rich in mint-condition and refined handaxes that large-scale excavation was carried out. Throughout 1995 and 1996, open-area excavation of over 501 m² was undertaken through English Heritage funding. The excavations recovered ca. 15,000 artefacts and ca.

12,000 pieces of mammalian fauna preserved as part of a complex series of spring-fed, freshwater deposits. The Q1/B location contains a spring-fed calcareous water body, revealing a generally wetter depositional environment (Pope 2002). This is a complex horizon that extends across the site and that Macphail described (Macphail 1996, 1999; Macphail and Goldberg 2017; Pope et al. 2020) through sediment micromorphological analyses. In paleogeographic terms, these deposits appear to represent a small freshwater lake within a grassland which formed after marine regression that led to the drying out of the intertidal silts (Unit 4b) and the initiation of soil formation and pedogenesis across the landscape (Roberts and Parfitt 1999). This grassland environment occupied a larger, 26 km-wide synclinal basin, fringed by degraded chalk cliffs and rich in nodular flint, with spring lines at their base (Roberts and Pope 2018). Q1/B is situated approximately 50 m to the south of the main west–east cliff line and consequently represents a location with affordances which may have been of value to the human groups using the landscape: fresh water, raw material for tools and cores,

meat procurement, shelter from northern winds and slopes with southerly aspects providing routeways to the chalk escarpment to the north of the site.

Full analysis of the sedimentary profile, paleoenvironment and human behaviour at the site has yet to be undertaken, but initial studies of site formation processes suggested a dynamic sedimentary environment which, in contrast to contemporary archaeological signatures from the wider grassland, had rearranged artefacts and faunal material to some degree (Pope 2002). In this study, the main freshwater units (Unit 3c, Unit 4/3, Unit 4u and Unit 4) were all shown to indicate varying degrees of post-depositional modification, but Unit 4u stood out, on the basis of refit distances and localised dense clusters of material, to represent a more minimally disturbed horizon with the possibility of the relatively high resolution of past human behaviour. The stone artefact assemblage from Unit 4u, upon which this study is focused, as with the other freshwater horizons, shared features which were distinctive when compared to the wider contemporary landscape signature, namely higher proportions of handaxes and flake tools (Pope 2002). Unit 4u lays at the base of the freshwater deposits (Fig. 2) at the site and has preserved 4653 stone artefacts > 10 mm in maximum dimension and 3182 faunal remains > 10 mm. The level also produced the two human incisors found in 1995, which have now been shown to have a morphological affinity with a population described as early Neanderthal from Sima de los Huesos (Atapuerca, Spain) (Lockey et al. 2022). This seems to be the only stratigraphic horizon where stone artefacts appear associated with pre-MIS12 hominin remains in northern Europe; therefore, it is important to test the integrity of that association. This study takes forward our understanding of this key horizon in order to establish the degree of post-depositional modification of the archaeological signature within Unit 4u and to help develop a methodological framework for taking forward the full analysis of this taphonomically complex but important locality of Q1/B.

Materials and methods

The data used for this study comes from excavations carried out between 1995 and 1996 in Unit 4u at the Q1/B site of Boxgrove (West Sussex, UK). The software used for the geostatistical analysis and spatial distribution patterns is ArcGIS 10.5. The materials and methods used for each of the variables are detailed below.

Palaeotopographic reconstruction

The reconstruction of Unit 4u was carried out with the aim of evaluating possible palaeotopographic constraints in the distribution pattern (Sánchez-Romero et al. 2020).

We applied a geostatistical procedure known as Kriging to 21,812 points taken with a centimetre accuracy GPS, with a constant distance between them of 0.15 m, and a radius of 8 sectors. Kriging is an interpolation method used for paleogeographic reconstructions (Oliver 1990), which has turned out to be a very useful resource for estimating the palaeosurface where materials were deposited and accumulated (Sánchez-Romero et al. 2021). In order to understand the depositional dynamics of the Unit 4u materials, we reconstructed the top of Unit 3, which constitutes the palaeosurface where Unit 4u materials lay.

Data spatial analysis

A range of statistical tests were applied to determine the distribution pattern. We applied both general tests to evaluate the type of distribution, such as average nearest neighbours (ANN), Ripley's K function or chi-squared and Kolmogorov–Smirnov (K-S); and local tests to locate the clusters, in case the pattern obtained in the previous tests indicated that the distribution is clustered. Regarding the general tests, ANN compared the observed and the expected mean distances (Getis 1964), to discriminate dispersed from clustered patterns. Ripley's K function (Ripley 1976) calculates the degree of clustering and how the dispersed or clustered elements vary in relation to the distance in the study area. Lastly, chi-square and K-S statistical tests were applied through quadrat method (Lee and Wong 2000) with the aim of identifying the clustered, dispersed or random nature of the whole assemblage. These tests were applied to a total of 1087 quadrats and 3549 points. The application of several tests in spatial and statistical studies reduces uncertainty, allowing us to verify and confirm specific results (Sánchez-Romero et al. 2021). Because none of these tests indicates the actual location of the clusters, it was then necessary to apply other local analytical methods. To locate these clusters, we applied hotspots methods, such as Getis-Ord G_i^* and Anselin Local Moran's I, which have turned out to be the most useful tools for the identification of local spatial clusters according to a quantitative variable (Sánchez-Romero et al. 2016, 2020; Mora Torcal et al. 2020). The main difference between them is that Anselin Local Moran's I identifies the atypical values, while Getis-Ord G_i^* evaluates the degree of clustering according to the statistical significance of high/low values excluding atypical values (Moran 1950; Getis and Ord 1992; Siabato and Guzmán-Manrique 2019; Sánchez-Romero et al. 2021). In this study, we handled a large sample size, with a total of $n = 4653$ lithic pieces and $n = 3182$ faunal remains, in which Getis-Ord G_i^* and Anselin Local Moran's I tests have been applied according to the variable of maximum dimension (MD). All the spatial relationships (fixed, inverse and inverse distance squared) showed similar results, but the inverse distance squared made it possible to better appreciate

Member	Description and interpretation	Standard	Q1/B	Description and interpretation
Eartham Upper Gravel	head gravels derived from downland Clay-with-flints regolith; mass-movement deposits, with arctic soils	Unit 11	Unit 11	head gravels from derived from downland Clay-with-flints regolith; mass-movement deposits, with arctic soils
	calcareous head; mass-movement deposit	Unit 10	Unit 10	calcareous head; mass-movement deposit
	path gravel; freeze-thaw-sorted flint gravel	Unit 9		
	Upper Chalk pellet gravel; waterlaid, weathered and sorted chalk clasts	Unit 8	Unit 8	Chalk pellet gravel; dewatering structures initiated
Eartham Lower Gravel	cliff collapse; Lower Chalk pellet gravel	Unit 7		
	calcareous muds/brickearth; colluvial and waterlaid silts	Units 5b, 6	Unit 6b	calcareous muds/brickearth; colluvial and waterlaid silts
Slindon Silt	mineralised and compressed organic deposits; alder/fen carr	Unit 5a	Unit 5a	mineralised and compressed organic deposits; alder/fen carr
	soil horizon developed on top of the silts; Polder-type soil	Unit 4c	4d2, 4d3, 5ac	spring discharge sediments with colluvial input towards the top (Unit 5ac)
	intertidal laminated muds laid down in a semi-enclosed marine bay	Unit 4b	Unit 4d1	spring discharge sediment; intraformational calcretes
		Unit 4	Unit 4	massive silt from freshwater reworking of Units 4a and 4b; heavily deformed
		Unit 4a	Unit 4u	massive fine silt from freshwater reworking of Units 4a and 4b; includes subunits 4u(s) and 4*
Slindon Sand	nearshore marine sands	Units 3/4, 3c		freshwater channels and freshwater scoured land surface, from springs at cliff base
		Unit 3	Unit 3	nearshore marine sands with a truncated upper surface

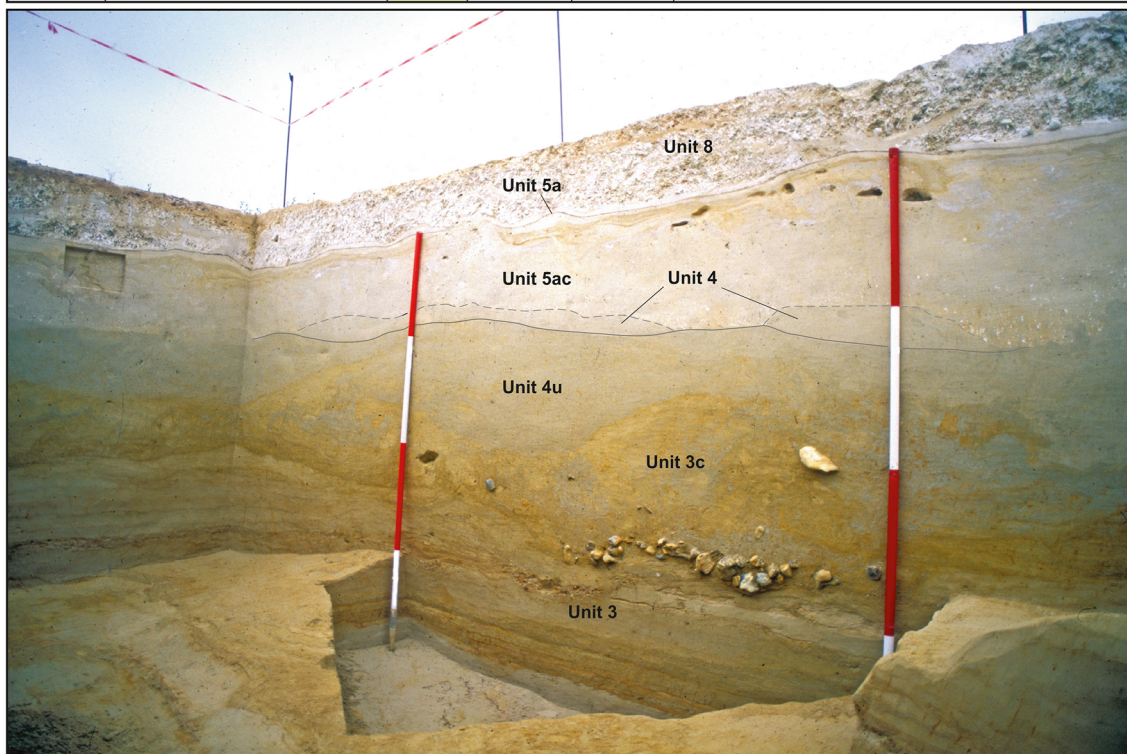


Fig. 2 Stratigraphic relationship between the Boxgrove sequence and that recorded at the Q1/B site (above) (Pope et al. 2020). Section of Trench 23 of Q1/B with the sequence of units labelled (below) (Roberts and Pope 2018)

the influence between neighbours. In the case of Anselin Local Moran's I , 99 permutations were performed.

In addition, Kernel density analysis (KDE) (Silverman 1986) was applied to obtain a simple and graphically visual projection of the accumulation zones. The search radius selected was 1 m, due to the area of the site and characteristics of the input data. The density map was classified into two classes by the Jenks method (Jenks 1967), to group similar values and maximize the differences between specified classes through the elimination of intermediate values. This classification provides a high-resolution estimation of zones according to their concentration of materials (Sánchez-Romero et al. 2016, 2020).

The characterization of the clusters and the materials that compose them was analysed in different ways. On the one hand, orientation patterns and 3D-fabric analyses (Bertran and Texier 1995; Bertran and Lenoble 2002; Benito-Calvo et al. 2009; De la Torre and Wehr 2018) were performed with the orientation and dip data of long axis calculated with compass and clinometer in the field (Pope 2002), whose validity has been demonstrated to infer possible post-depositional disturbances and their impact degree on the assemblage (Chu and Hosfield 2020). Thus, the analysis of orientation and slope patterns was carried out with those materials with the longest axis clearly identifiable (Lenoble and Bertran 2004), including both lithic and faunal remains. The total sample size for lithic ($n = 1294$) and faunal ($n = 772$) remains is wide, which has provided reliable statistical results. The orientation patterns have been calculated through the analysis of the angular histograms together with different statistical tests, in this case considering only azimuthal data ($0\text{--}360^\circ$). The reason for using only azimuth angles instead of axial ($0\text{--}180^\circ$) and azimuth angles is because the materials were recorded using a compass, which is aligned with the longest axis of the piece taking the azimuth in the direction marked by the slope of the piece (Sánchez-Romero 2019). The axial angles are useful when slope data are not available and when only information about the orientation of the materials is available, such as drawings (Sánchez-Romero et al. 2016). The statistical analysis has been performed with the Rayleigh and Kuiper tests, which allow differentiating isotropic distributions (uniform) from unimodal, bimodal or multimodal patterns (Benito-Calvo and De la Torre 2011; De la Torre and Benito-Calvo 2013; Sánchez-Romero et al. 2016). On the other hand, shape patterns (Sneed and Folk 1958; Benn 1994; Ringrose and Benn 1997; Benn and Ringrose 2001) of lithic and fauna remains have been calculated (Roy Sunyer et al. 2014; Sánchez-Romero et al. 2020, 2022; De la Torre et al. 2021), with the aim of knowing the cluster composition and to see if any shape selection exists in the distribution of materials.

Archaeostratigraphy

The archaeostratigraphic method was applied in order to analyse the vertical distribution of materials (Stein and Deo 2003; Canals et al. 2003; Bargalló et al. 2016, 2020; Sánchez-Romero et al. 2017; Mora Torcal et al. 2020; Spagnolo et al. 2020, *inter alia*). This makes it possible to observe vertical variations in the distribution of materials and detect possible hiatuses, which could indicate the presence of several episodes of deposition of materials not identifiable in the stratigraphy. The archaeostratigraphic profiles were delimited every 2 m and have enabled us to analyse the distribution pattern of the materials, from the bottom to the top of Unit 4u.

Refitting analysis

Refitting studies are not common in open-air deposits, since most of them are in caves, with rare exceptions (Bourguignon et al. 2002; Clark 2017; Pope et al. 2020). Thus, the spatial analysis of the Q1/B open-air site, considering and integrating a large number of refits, makes it even more important to address the formation processes discussed and understand the complexity of this type of study in open-air sites.

A pilot system of refitting analysis was undertaken as part of the analysis to date. It consisted of initial groupings of raw material types for the whole site, to provide an initial indication of refit distances and the presence and scale of refits between sedimentary units (using the “Cziesla approach”, *cf.* Cziesla 1986, 1990; De Loecker 2004). Compared to the focus and systemic refitting processes for the Boxgrove Horse Butchery Site (GTP17, Pope et al. 2020), the scope and scale of the refitting program are limited. This refitting analysis was performed to control the most dynamic part of a spatial analysis (Romagnoli and Vaquero 2019), since it allows evaluating of movements and displacements of the pieces, either by natural processes or by activities developed by humans. Thus, a total of 206 refitted pieces and 198 refitting lines were used to calculate the orientation patterns and 3D fabric analysis (De la Torre et al. 2018). Each refit comprises two conjoined flint artefacts or fragments of flint artefacts, with a clear predominance of flakes, almost 90% (89.86%, $n = 186$). The results have been compared with those obtained in the analysis of lithic and faunal remains as independent assemblages.

Results

Palaeotopography

The continuous high-resolution surface interpolated for the base of Unit 4u is shown in Fig. 3. It is possible to observe up to a metre of topographic variation between the highest and lowest parts of the underlying surface (profile A-A').

The total reconstructed area covers around 485.30 m² and shows two topographic lows, one to the south-west and the other to the south-east, forming distinct basins a few metres across which appear to be confluent at the extreme south end of the excavation area (Fig. 3). The basin located at the southeastern sector (SEB) shows a N-S direction and an area of roughly 93 m². In this basin is where most of the faunal and artefacts assemblages were concentrated. The southwestern basin (SWB) covers around 122 m² and has a NW–SE alignment. These basins are delimited by more elevated areas (ridges), located at the northeastern (NER) and centre part (CR), and where Unit 4u was sparsely present or absent in these more elevated areas.

Cluster identification

The ANN results indicated, for both lithic and faunal distributions, that the observed average distance of the projected materials is clearly lower than we would expect in a hypothetical random distribution, indicating that the remains are clustered (Table 1). The z-scores show that there is less than a 1% likelihood that this pattern could be the result

Table 1 Statistical results obtained from the application of ANN and Ripley’s K function statistical methods

	Fauna	Lithics
Average Nearest Neighbor (ANN)		
NN observed	0.12	0.11
NN expected	0.21	0.36
NN ratio	0.58	0.3
NN z-score	−44.75	−91.71
p-value	0	0
Ripley’s K Function		
Maximum difference observed-expected	2.63	10.85

of random chance. Ripley’s K function indicates more neighbours than could be expected in a random pattern, the empirical curve (observed) being higher than the theoretical one (expected). This is consistent with a clustered pattern for both variables. These results have been ratified by the application of chi-square and K-S tests by quadrats (Lee and Wong 2000), which indicated a clustered pattern where both critical values are lower than the significance level ($p=0.95$) ($K-S=0.404 > 0.032$; $X^2(25)=2.81E+22 > 37.652$). These

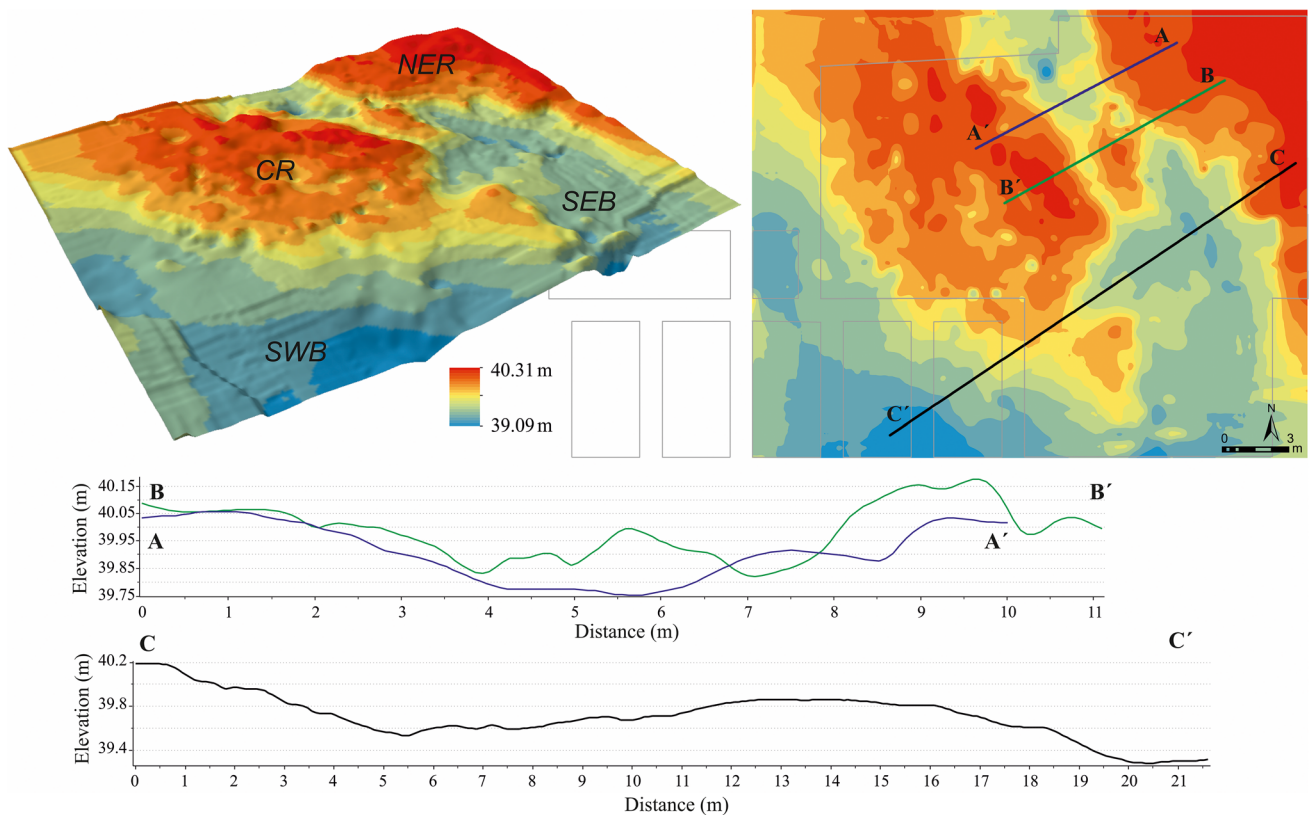


Fig. 3 3D and 2D palaeotopographic reconstruction of the Unit 4u base at the Boxgrove Q1/B site and morphological profiles. These morphological profiles indicate the variations on the palaeotopography at different parts of the reconstructed area. The variation in eleva-

tion barely reaches 0.5 m in profiles A–A’ and B–B’, and less than a metre in the longest profile (C–C’). The grey lines indicate the limits of the excavation

results allow us to reject the null hypothesis of a random distribution. The results obtained through KDE using the Jenks classification show that materials, both lithic and fauna, are mainly accumulated in the southeastern part of the excavated area (Fig. 4), in the SEB sector, comprising an area of approximately 46 m². However, towards the west of the main accumulation, there are also some patches of accumulation of material.

With the aim of determining the statistical significance of zones highlighted as being the densest, Getis-Ord Gi* (fixed) was applied to the variable of nearest neighbours. This analysis indicated that the main accumulation zones detected by KDE and classified by Jenks showed a 99% statistical significance. This classification showed that the zone located in the SEB sector contains the largest concentration of remains (Fig. 5), indicated by the higher values of nearest neighbours. However, other concentrations highlighted

by KDE and Jenks in other sectors, like SWB, are classified as coldspots, indicating lower values of nearest neighbours, and hence less concentration of materials in these sectors of the site. These clusters of hotspots according to the number of nearest neighbours (or materials) were named NML and NMF, both for lithics and fauna respectively.

In order to evaluate any pattern related to the material dimensions, Getis-Ord Gi* and Anselin Local Moran's I stats were also applied according to the MD variable. Getis-Ord Gi* analysis showed that there are several clusters of high and low MD values, which are mainly located in the extremes of the maximum concentration of materials (NML and NMF). For the lithic industry, the main MD hotspot cluster (HL1) is well-delimited at the southeast (Fig. 6) and constitutes 283 pieces, with 99% confidence, while the main MD coldspot cluster (CL3) is located at the north and comprises 353 pieces, with 95–99% confidence. Apart from

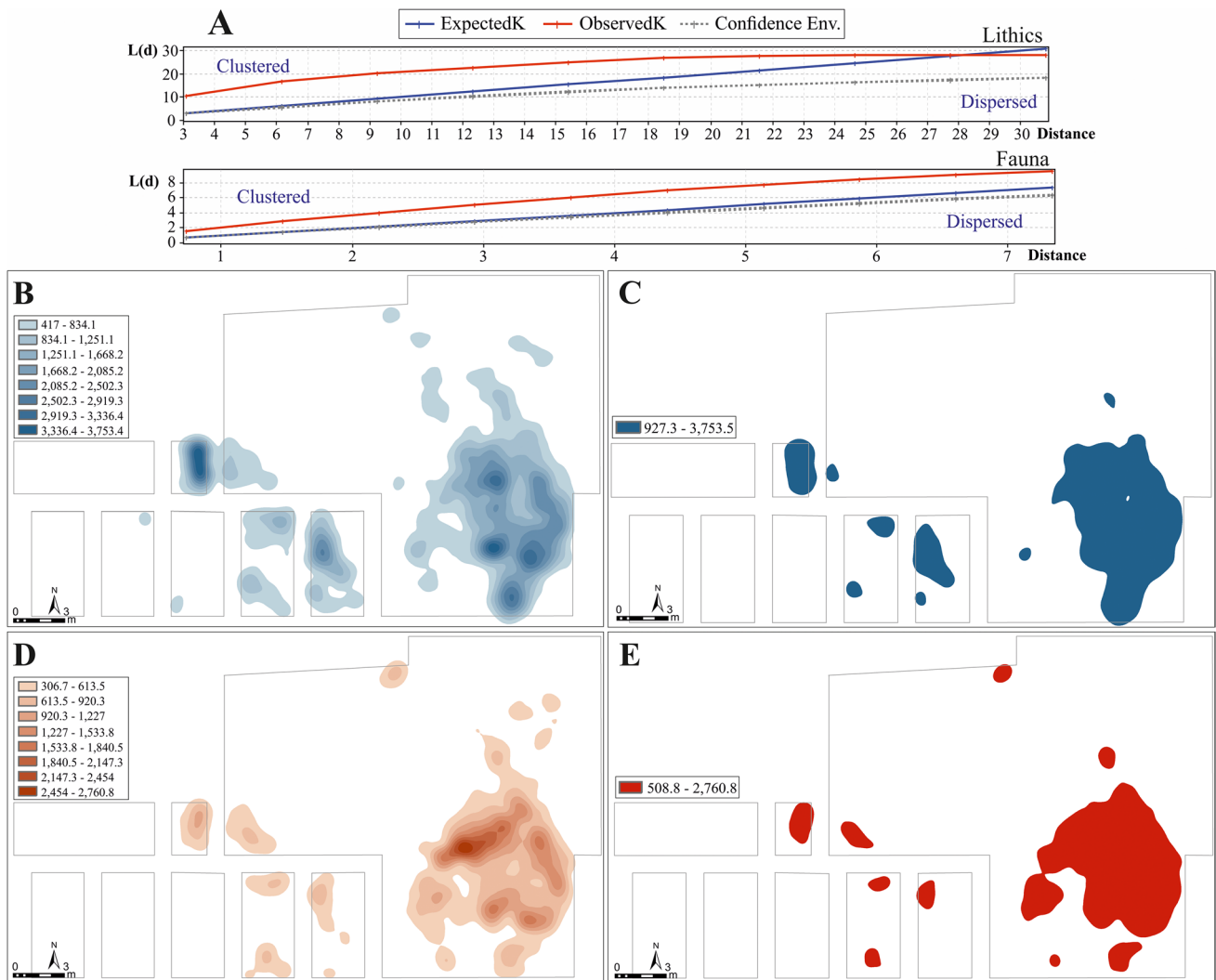
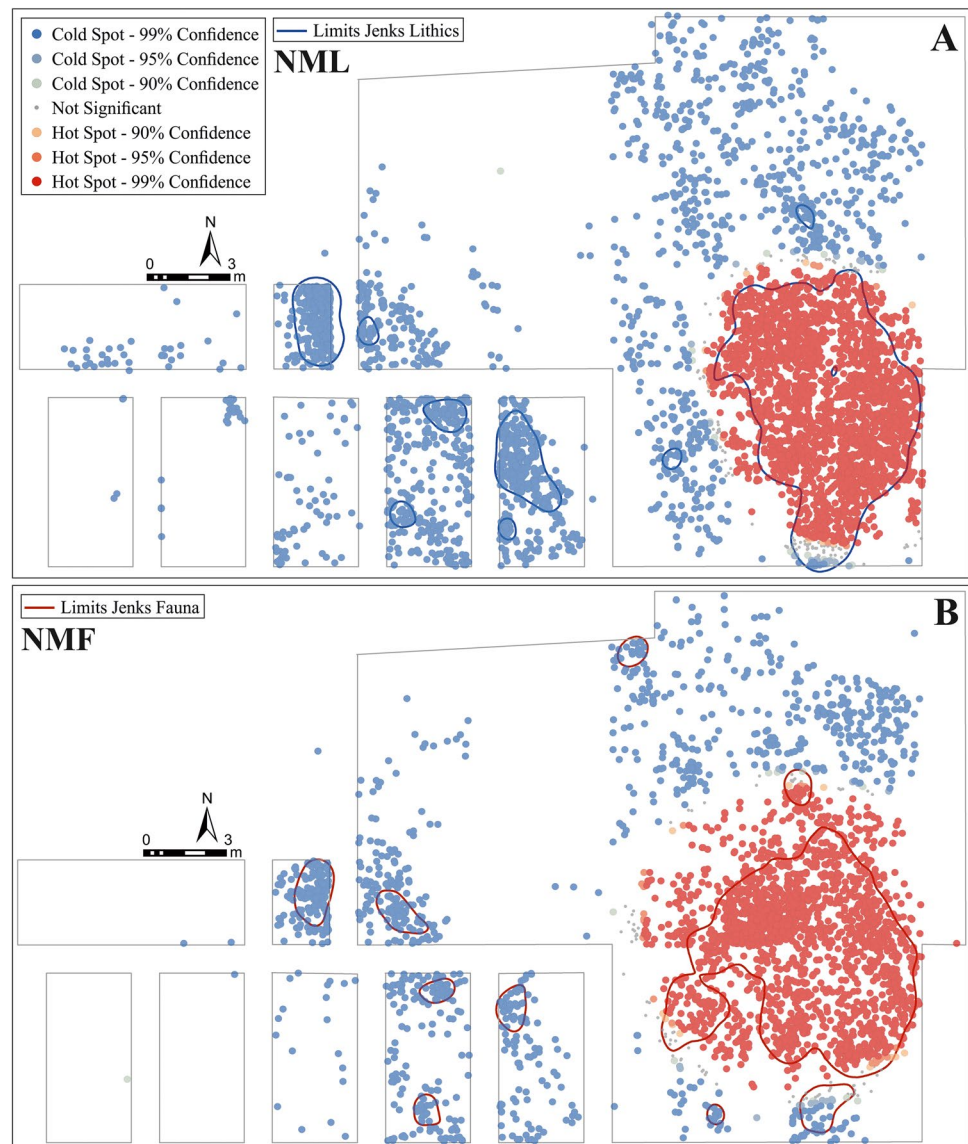


Fig. 4 A Ripley's K function graphics confirming the clustered nature of the bone and lithic assemblages. KDE density map (B) and Jenks classification (C) for lithic materials. KDE density map (D) and Jenks classification (E) of bones

Fig. 5 Getis-Ord G_i^* applied to the variable of nearest neighbours in lithics (**A**) and bones (**B**). The line (blue in **A** and red in **B**) indicates the limits marked by the Jenks classification density analysis (see Fig. 4)



these clusters, there are other more dispersed and smaller MD clusters, of both high and low values (Fig. 6). There are two more lithic clusters highlighted as hotspots and coldspots towards the NER sector, with a scattered distribution and lower statistical significance (95–99% confidence).

The analysis of the bone assemblage has allowed the identification of several MD hotspot and coldspot clusters. The main MD bone hotspot cluster (HF1) is also located at the southeast, like in the case of lithics (Fig. 6), and it is formed by 725 remains. The main MD bone coldspot cluster (CF1) is more dispersed than the coldspot cluster identified for lithic materials (Fig. 6), but it is also in the northern part of the excavated area. This cluster comprises 703 remains, very similar to the hotspot cluster.

In general, the same MD clusters are identified by Getis-Ord G_i^* and Anselin Local Moran's I, but the latter test

allows evaluating of some details about the clustering and data. In the case of lithic materials, the main MD coldspot cluster (CL3) is identified as a cluster mainly composed of low values, but there is a large number of atypical high values surrounded by low values (red). Likewise, the main MD hotspot cluster (HL1) also shows many atypical low values surrounded by high values (dark blue) (Fig. 6). Although both tests usually identify the same clusters, Anselin Local Moran's I allows evaluating the percentage of atypical values in clusters mainly classified as hotspots or coldspots.

When we turn to the orientation patterns and fabric analysis for all items, the results obtained for the whole lithic assemblage ($n = 1294$) indicate low p -values for the Rayleigh and Kuiper (Table 2), which clearly reject uniformity, and point to a dominant unimodal pattern for this assemblage. The histogram shows a clear trend to the north,

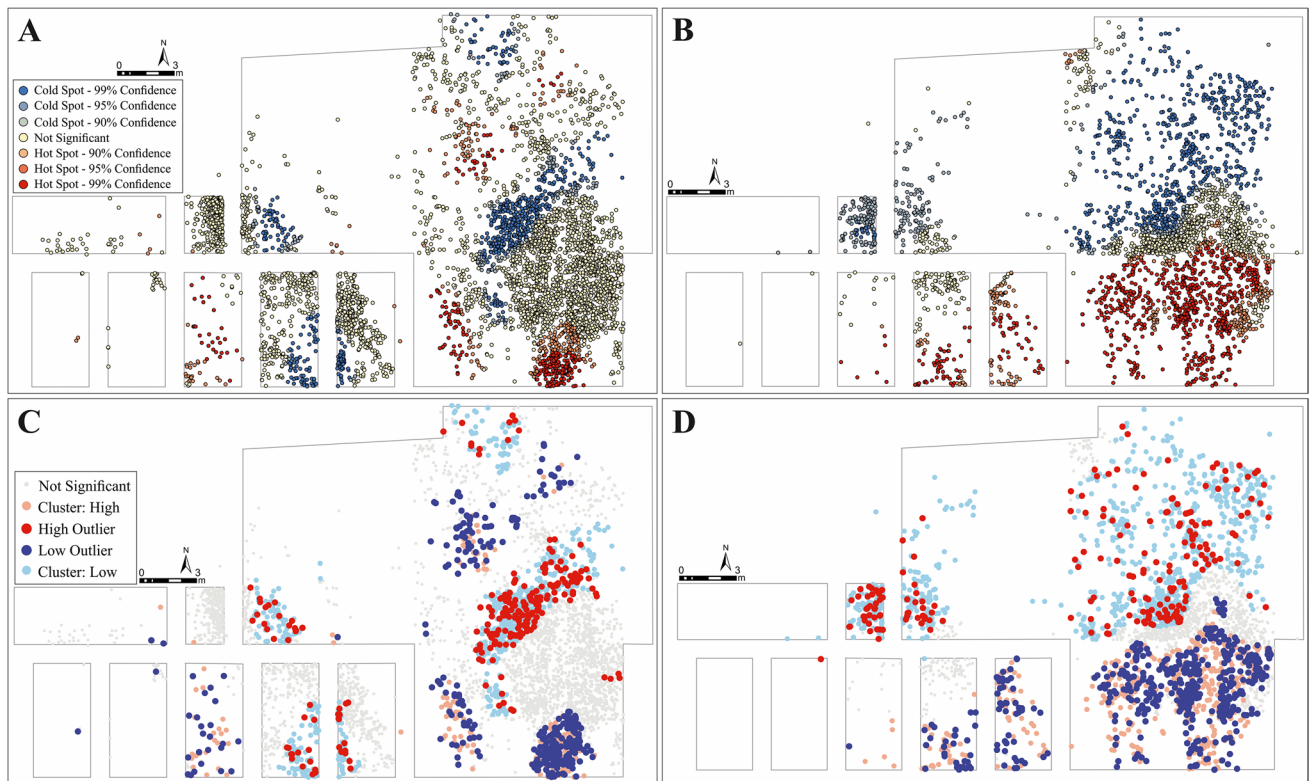


Fig. 6 Getis-Ord G_i^* applied to lithics (A) and bones (B). Anselin Local Moran's I applied to lithics (C) and bones (D)

in a kind of fan-like shape graphic (Fig. 7), and a minor E-W mode.

The data on the bone assemblage ($n = 772$) and the Rayleigh and Kuiper p -values also point to a dominant unimodal pattern (Fig. 7), indicating a main NNW alignment, besides other minor modes (Fig. 7). Additionally, 3D-fabric analysis has allowed observation of differences between lithic and bone assemblages (Fig. 8, Table 3), with lithic materials showing a greater trend to isotropy than bones, whose trend is towards a planar fabric. Eigenvalues and Benn's projection delve into the characteristics of the assemblages. Both variables are situated in the left side of the triangle, far from isotropic and linear fabrics, suggesting a mostly planar fabric for these assemblages. The features are coherent with the other values analysed for these groups, such as the low values for the isotropy parameter ($I = 0.476$ for lithics and $I = 0.256$ for fauna) and the very low elongation of the

fabrics ($E = 0.032$ for lithics and $E = 0.098$ for fauna), which indicate that there does not seem to exist any shape pattern in the accumulation of these assemblages. The K index (Woodcock 1977) allows the distinction planar ($0 < K < 1$) from linear ($1 < K < \infty$) fabrics, and also shows low values for both variables (Table 3). The parameter to calculate the horizontal index (F) shows higher values, especially for lithics, confirming this planar trend.

Clusters description

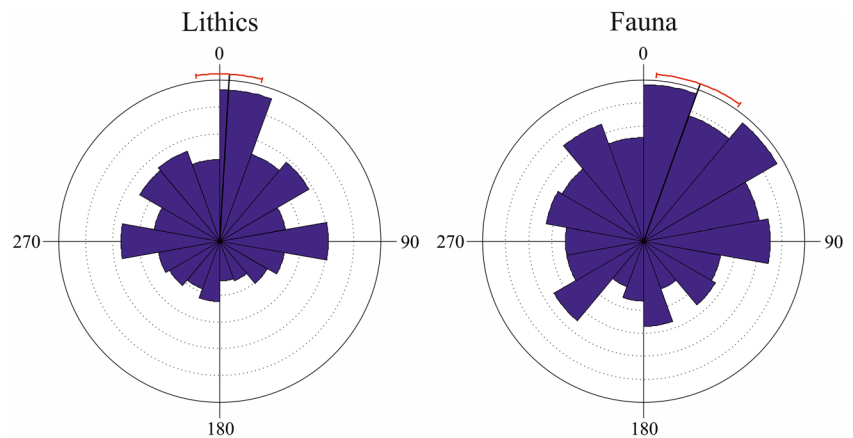
Clusters by number of neighbours

Clusters identified according to the number of nearest neighbours are well delimited in the SEB sector for both variables, remaining practically within the limits of this basin. The NML cluster is composed of 2328 lithic remains, although

Table 2 Dispersion patterns and statistical tests of the lithic and fauna assemblages of Q1/B site

	Sample size <i>n</i>	Method	Mean vector (°)	Length of mean vector	Concentration	Circular standard deviation (°)	Rayleigh test		Kuiper's test	
			μ	<i>r</i>	<i>k</i>	<i>v</i>	<i>Z</i>	<i>p</i>	<i>V</i>	<i>p</i>
Lithics	1294	Azimuth	3.258°	0.191	0.388	104.322°	47.008	<1E-12	5.42	<0.01
Fauna	772	Azimuth	20.053°	0.186	0.378	105.141°	26.616	2.76E-12	3.974	<0.01

Fig. 7 Circular histograms of the orientation patterns of lithic and fauna assemblages of the Boxgrove Q1/B site



only 644 items had orientation data. The mean size is 38.07 mm, with 11 mm as the minimum and 190 mm as the maximum length. In the case of NMF, it is composed of 1943 faunal remains, although, as in the case of NML, 692 had orientation data. The mean length for the bones of this cluster is 30.94 mm, varying between a minimum of 9 mm and a maximum of 540 mm. The limits of both hotspots are circumscribed to those set by the Jenks classification, although with differences in the smaller accumulations. In terms of orientation patterns, both clusters have a similar sample size, which enables a good comparison between them. NML and NMF have identical data for Rayleigh and Kuiper's tests, indicating very low *p*-values and pointing to a clear multimodal pattern (Table 4). These data are coherent with the histogram obtained for them both. The shape seems to be homogeneous, but we can observe clear directional trends towards NWN-W for NML and N-E for NMF (Fig. 9). Both histograms are very similar to those obtained for the assemblages of lithics and fauna (Fig. 7).

Clusters by maximum dimension (MD)

Besides the clusters identified according to the number of nearest neighbours, we have detected several significant

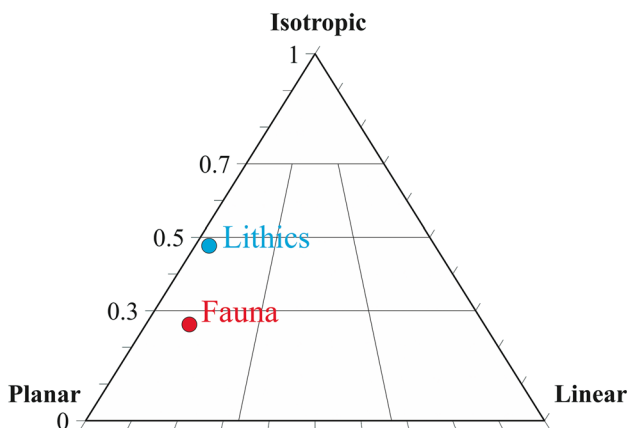


Fig. 8 Benn's fabric diagram with the 3D-fabrics for lithics and bones

concentrations of high and low values relating to the maximum dimension of each item. In the case of lithic materials, five MD clusters have been detected (Fig. 10), both hotspots and coldspots. The main MD clusters partially coincide with the main accumulation defined by the number of materials (NML), while the rest of the MD clusters are close or even out of these limits (Fig. 10). The number of elements contained in each cluster varies, as well as the length according to their classification as hotspot or coldspot. The mean length for hotspot clusters is 40–50 mm, with a minimum length of 20 mm and maximum close to 200 mm. In the case of coldspot clusters, the mean is around 35 mm, while the minimum is 20 mm and the maximum between 100 and 132 mm (Table 5).

Regarding orientation patterns, the number of pieces is slightly lower than the actual number of pieces contained in each cluster, since not all have orientation data. The larger cluster is CL3 with 187 pieces (Table 6), while the rest of the sample sizes are too small to be considered when reaching any conclusion about orientation patterns (Ringrose and Benn 1997; Benn and Ringrose 2001; McPherron 2018). Thus, only CL3 has been considered for the analysis of lithic assemblage. The results obtained indicate a clear orientation of materials, with low *p*-values of both Rayleigh ($p = 5.62E-08$) and Kuiper ($p < 0.01$) (Table 6). The histogram shows a mainly unimodal pattern that points in a NNE direction (Fig. 10), very similar to the graph obtained for the whole lithic assemblage.

In relation to the fauna assemblage, fewer MD hotspot and coldspot clusters have been detected than in the case of the lithic industry. Only four MD clusters have been identified (Fig. 11), with CF1 ($n = 703$) and HF1 (main, $n = 725$) being the larger ones, and hence those selected for the study (Table 7). These clusters partially coincide with the NMF cluster, and the zones delimited by KDE and Jenks, but, in contrast to lithic assemblage, in this case, there are greater coincidences with the limits marked by KDE and Jenks. The mean length for hotspot clusters is around 40 mm, with a minimum fixed of 5 mm and a

Table 3 Eigenvalues with the 3D fabric indexes corresponding to lithic and bone assemblages according to the Benn (1994) method. K and C parameters have been calculated according to Sneed and Folk (1958). C.L. refers to the confidence level

		Lithics (n=1033)	Fauna (n=770)
E1	Azimuth	237.16	49.38
	Plunge	9.36E+01	2.29
	Eigenvalue	422,595	356,835
E2	Azimuth	327.16	319.34
	Plunge	3.35	0.84
	Eigenvalue	409,088	321,919
E3	Azimuth	147.00	209.17
	Plunge	86.65	87.56
	Eigenvalue	201,318	91,246

	K	C	I	E	F	C.L
Lithics	0.046	0.742	0.476	0.032	0.492	>99%
Fauna	0.082	1,364	0.256	0.098	0.283	>99%

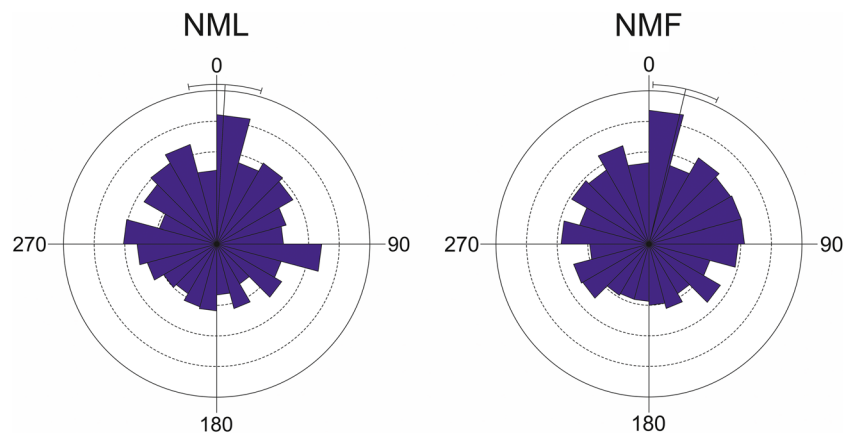
maximum between 190 and 200 mm (Table 7). The coldspot clusters show a mean length of 20–25 mm, with 1 mm as minimum and 110 and 250 mm as maximum length.

There are large differences between hotspot and coldspot clusters, not only in mean sizes but also in terms of minimum lengths.

Table 4 Statistical tests and dispersion parameters of NML and NMF clusters

	Sample size <i>n</i>	Method	Mean vector (°) <i>μ</i>	Length of mean vector <i>r</i>	Concentration <i>k</i>	Circular standard deviation (°) <i>v</i>	Rayleigh test		Kuiper's test	
							<i>Z</i>	<i>p</i>	<i>V</i>	<i>p</i>
NML	644	Azimuth	3.046°	0.234	0.481	97.697°	35.171	<1E-12	4.23	<0.01
NMF	692	Azimuth	13.385°	0.249	0.514	95.579°	42.81	<1E-12	4.769	<0.01

Fig. 9 Circular histograms of the orientation patterns for NML and NMF clusters



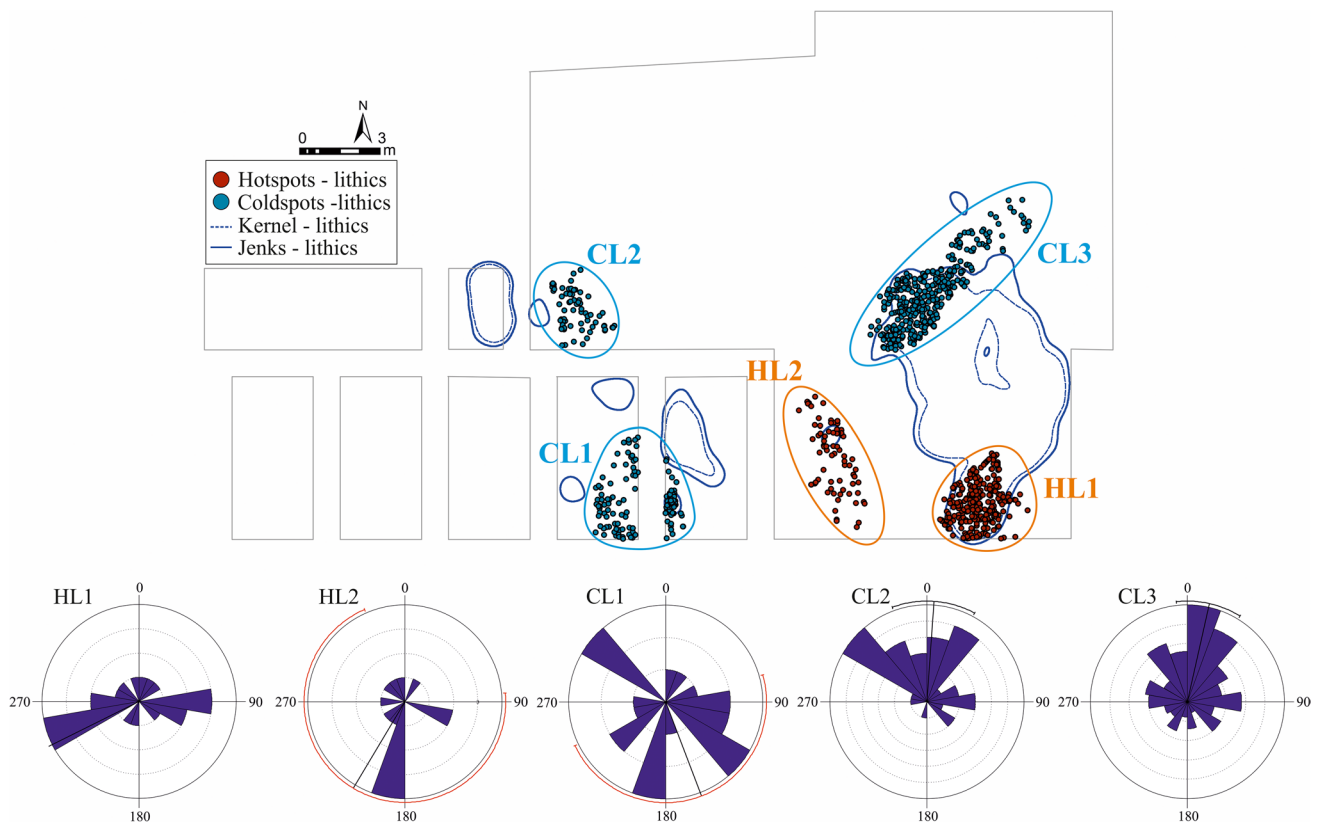


Fig. 10 Classification and delimitation of the clusters of lithic materials identified by Getis-Ord G_i^* , and the circular histograms associated to these clusters. The solid line indicates the limits marked by

the Jenks classification and the dashed line the limits marked by KDE, both for lithics (see Fig. 4)

The clusters with larger sample sizes are CF1 ($n=245$) and HF1 ($n=195$). In both clusters, p -values are low, indicating a clear preferred orientation pattern (Table 8). The histogram of CF1 shows a unimodal pattern towards the N, defined by a fan-like shape varying from NW to NE (Fig. 11), similar to that observed in cluster CL1 for lithic materials. The histogram obtained for the HF1 cluster tends towards the E or ENE, a direction that has been also observed in HL1.

Refitting dynamics

The total number of refitting lines is 198, of which 16.16 ($n=32$) are shorter than 1 m in length and 9.09% ($n=18$) are longer than 7 m (Table 9). There are 40

refitting lines of 1–2 m in length, representing 20.20% of the total. This implies that this distance is the most common among all the refitting lines for Q1/B. Experimental studies indicate that the flakes produced by a standing knapper hardly move more than 2 m (Schick 1986). The percentage of pieces moved more than 2 m is low, but due to the fact that there are also very long refitting lines on the site, we cannot consider that some refitting sequences were not subject to the action of postdepositional processes. Several lines reach some metres in length, such as the longest line located at the south of the site, which runs E-W and is 23.52 m (Fig. 12). Also, there is a refitting line of a NE direction, whose length (16.02 m) is similar to another long line located at the east (12.76 m), very close to the longest one. The 3D representation of palaeotopography together with refitting lines (Fig. 12) allows an appreciation of how most refits are limited to the basin located at the south of the excavated area, with a few refitting lines connecting to other areas. Any lines that extend outside of the basins show longer lengths.

The distribution analysis of refitting lines indicates that most of them are concentrated in the SEB sector, where the

Table 5 Number of lithic pieces contained in each cluster; mean, minimum and maximum length for each of them (in millimetres)

	<i>n</i>	Mean	Min	Max
HL1	283	42.5	20	197
HL2	72	52.55	22	143
CL1	130	32.2	18	102
CL2	69	35.42	20	119
CL3	353	35.88	18	132

Table 6 Statistical tests associated to the circular histograms of the identified clusters for lithic materials

Sample size	Method	Mean vector (°)	Length of mean vector	Concentration	Circular standard deviation (°)	Rayleigh test		Kuiper's test		
						Z	p	V	p	
n		μ	r	k	v					
HL1	20	Azimuth	243.502°	0.056	0.112	137.606°	0.063	0.941	1.092	>0.15
HL2	13	Azimuth	210.73°	0.256	0.24	94.564°	0.853	0.434	1.341	>0.15
CL1	21	Azimuth	159.285°	0.202	0.412	102.496°	0.856	0.43	1.055	>0.15
CL2	34	Azimuth	4.005°	0.522	1.219	65.323°	9.267	5.25E-05	2.462	<0.01
CL3	187	Azimuth	12.637°	0.299	0.626	89.058°	16.694	5.62E-08	2.977	<0.01

main accumulations of materials are also located (Fig. 12). Refitting density maps reflect that most of the refitting lines join in a SE zone of the main accumulation area (SEB sector), showing an elongated distribution pattern for the maximum density zone with a N-S axis, as well as an area of medium densities prorogued towards the W (Fig. 12). Apart from that main density area, there is a minor concentration of refitting lines at the centre-south, which coincide with the CL1 cluster detected in the lithic assemblage according to the MD variable.

In terms of refitting orientation patterns, Rayleigh and Kuiper's statistical tests indicate a clear oriented pattern, with low p -values for both tests (Table 10). Besides, the histograms show a pattern clustered to N and W directions (Fig. 13, Table 10). The 3D-fabric analysis points to planar fabric (Fig. 13), indicating that most of the refitting lines do not experience great variations in Z , but rather they remain mostly planar and without significant differences in their slope.

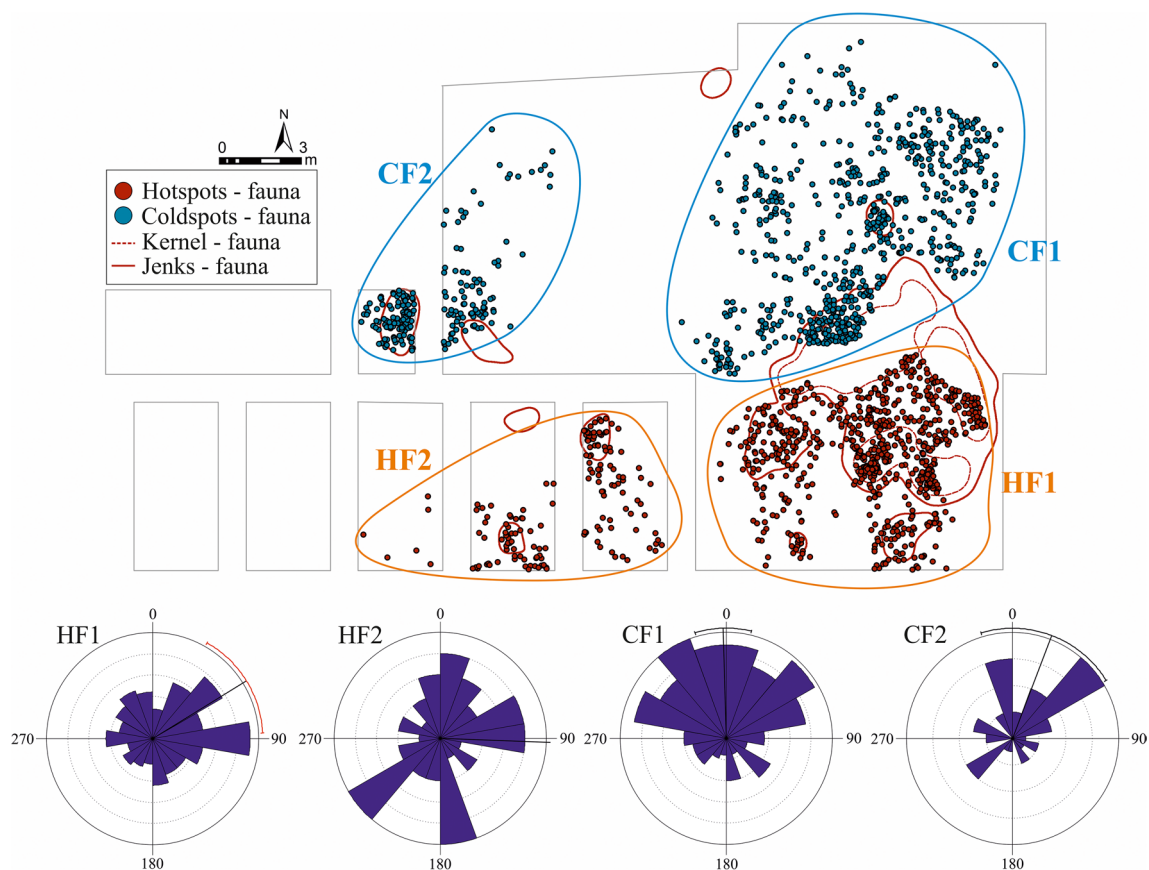


Fig. 11 Classification and delimitation of the clusters of bones identified by of Getis-Ord G_i^* , and the circular histograms associated to these clusters. The solid line indicates the limits marked by the Jenks

classification and the dashed line the limits marked by KDE, both for bones (see Fig. 4)

Table 7 Number of faunal remains contained in each cluster; mean, minimum and maximum length for each of them (in millimetres)

	<i>n</i>	Mean	Min	Max
HF1	725	38.4	5	200
HF2	159	39.96	5	190
CF1	703	21.69	1.2	250
CF2	203	24.93	1	110

Archaeostratigraphic analysis

The archaeostratigraphic analysis has allowed us to observe that the materials are more densely concentrated at the base of Unit 4u (Fig. 14), while at the top they are more dispersed. In general terms, the presence of continuous hiatuses in the deposition of the archaeological material has not been possible to identify, except for the identification of a possible discontinuous hiatus in a certain sector of the site (Fig. 14). The profiles where we detected a clearer identification of these hiatuses are D, E and F (Fig. 14), in which we can identify an empty layer separating two moments of deposition of materials. It is also possible to observe a change in the deposition dynamics as we analyse the profiles towards the north. The materials remain more concentrated both in the base and in the upper part of profile D, but towards the north the materials appear dispersed, especially in the upper part of the profile (see profile F). The profiles located towards the south show that materials are more concentrated, so we cannot make any distinction about hiatuses or differences in the deposition of materials.

Discussion

The palaeotopographical reconstruction of the Boxgrove Q1/B Unit 4u floor offers an integrated approach to reconstructing the context of the archaeological materials associated with this unit. The main accumulation is located in the wider basin situated towards the SE of the reconstructed area (SEB sector), which could suggest that the distribution was constrained by the paleotopography of the unit. We interpret the topography of Unit 4u as the eroded surface of Unit 3. Above this unconformity, the freshwater Unit 4u was emplaced, along with archaeological materials, filling both

localised scour hollows and larger basins. Consequently, the palaeotopography could be caused by erosional processes related to the erosion of the underlying Unit 3 surface, generating scours that were subsequently filled by sediments and archaeological materials from Unit 4u. In this way, the low energy flow of Unit 4u could have followed the erosion affecting the top of Unit 3, adopting a similar morphology in the first stages. The Unit 4u is a deposit composed of fine sediments, without channel facies, and with only occasional pebbles that do not point to any higher energy flow.

In searching for explanations to account for the movement of material, we have not detected the presence of channels which may have brought elements from the vicinity into the basins, as has been observed in other open-air sites, such as Ambrona (Sánchez-Romero et al. 2016). Nevertheless, the abundance of ostracods and fish remains indicates that Unit 4u is a freshwater deposit (Whittaker and Parfitt 2017), possibly fed by springs to the north of the site. Consequently, we might envisage either surface water flow or the rising water levels in a freshwater body during rainy seasons. This erosive episode could have been responsible for the denser concentration of materials at the base of the unit, as we observed in the archaeostratigraphic profiles. In the case of the lithic industry, the pieces do not show signs of roundness or alterations produced by high-energy processes, but rather they are exceptionally preserved (Roberts and Parfitt 1999; García-Medrano et al. 2019), even the smallest remains, such as debitage, debris and < 1 cm flakes (Wenban-Smith 1989; Roberts and Parfitt 1999; Stout et al. 2014).

The spatial analysis performed has enabled us to observe that the materials are mainly distributed in the lower parts of the reconstructed palaeotopography related to the base of Unit 4u, which rests on Unit 3 through a disconformity that could have redeposited Unit 3 and eroded margins of intact intertidal Unit 4B into Unit 4u. In the overall distribution, it is possible to distinguish the concentrations highlighted by KDE analysis, as zones of maximum concentration of materials, and by hotspot analyses, which indicate the clustering of low and high values. The principal concentrations of lithics (NML) and bones (NMF) are located in the SEB sector, where the main hot and cold spots according to the maximum length variable are highlighted. The general trend for lithics and

Table 8 Statistical tests associated to the circular histograms of the identified clusters for bones

	Sample size <i>n</i>	Method	Mean vector (°) μ	Length of mean vector <i>r</i>	Concentration <i>k</i>	Circular standard deviation (°) <i>v</i>	Rayleigh test		Kuiper's test	
							<i>Z</i>	<i>p</i>	<i>V</i>	<i>p</i>
HF1	195	Azimuth	58.277°	0.196	0.399	103.474°	7.475	5.67E-04	2.308	<0.01
HF2	46	Azimuth	92.169°	0.055	0.111	137.911°	0.14	0.87	0.872	>0.15
CF1	245	Azimuth	358.36°	0.331	0.702	85.198°	26.847	2.19E-12	4.143	<0.01
CF2	43	Azimuth	24.249°	0.324	0.686	85.963°	4.528	0.01	1.93	<0.025

Table 9 Distance ranges of the refitting lines (in metres) and number of refits in each range, as well as the percentage they represent with respect to the total number of refits

Length (m)	<i>n</i>	%
<0.5	13	6.57
0.5–1	19	9.60
1–2	40	20.20
2–3	35	17.68
3–4	23	11.62
4–5	25	12.63
5–6	14	7.07
6–7	11	5.56
7–8	3	1.52
8–9	5	2.53
9–10	3	1.52
>10	7	3.54
TOTAL	198	100

bones is to the north, with minor modes to the WNW and NEE in the case of the NML and NW-NE for NMF. However, when the clusters CL3, CF1 and HF1 are compared, we can observe some differences. In the case of CL3, the orientation pattern is very similar to NML, since the main direction is NNE and a mode to E. On the other hand, in the case of CF1, the direction is a fan-like shape that

points from WNW to NNE, while HF1 clearly shows an E main vector and a mode towards NE.

The orientation patterns for refitting lines show two main modes that point to the north and to the west (Fig. 13). In this sense, the tendency is more similar than those observed in the lithic clusters located at the south, something that seems to match with the fact that part of the main concentration of refitted pieces partially coincides with the main hot-spot cluster for lithic materials. Additionally, the 3D-fabric analyses performed for these variables (lithic pieces, fauna and refits) show that all have a mostly planar fabric, but with differences between them. The fabric obtained for refitting lines is clearly planar, located in the lower-left corner of the diagram (Fig. 13). However, and although fabrics of bones and lithics are also on the planar side, their trend points to certain isotropy, especially in the case of lithic materials (Fig. 8).

Consequently, two clear trends differentiated by the position of the materials in the Boxgrove Q1/B area have been detected. It is possible that the materials with a N-S trend in their orientation pattern are influenced by the palaeosurface morphology, as the azimuthal data of lithics and bones seem to indicate. However, the materials that show an E-W trend, located at the southern part of the reconstructed area, might have also been conditioned by the palaeorelief, but with the

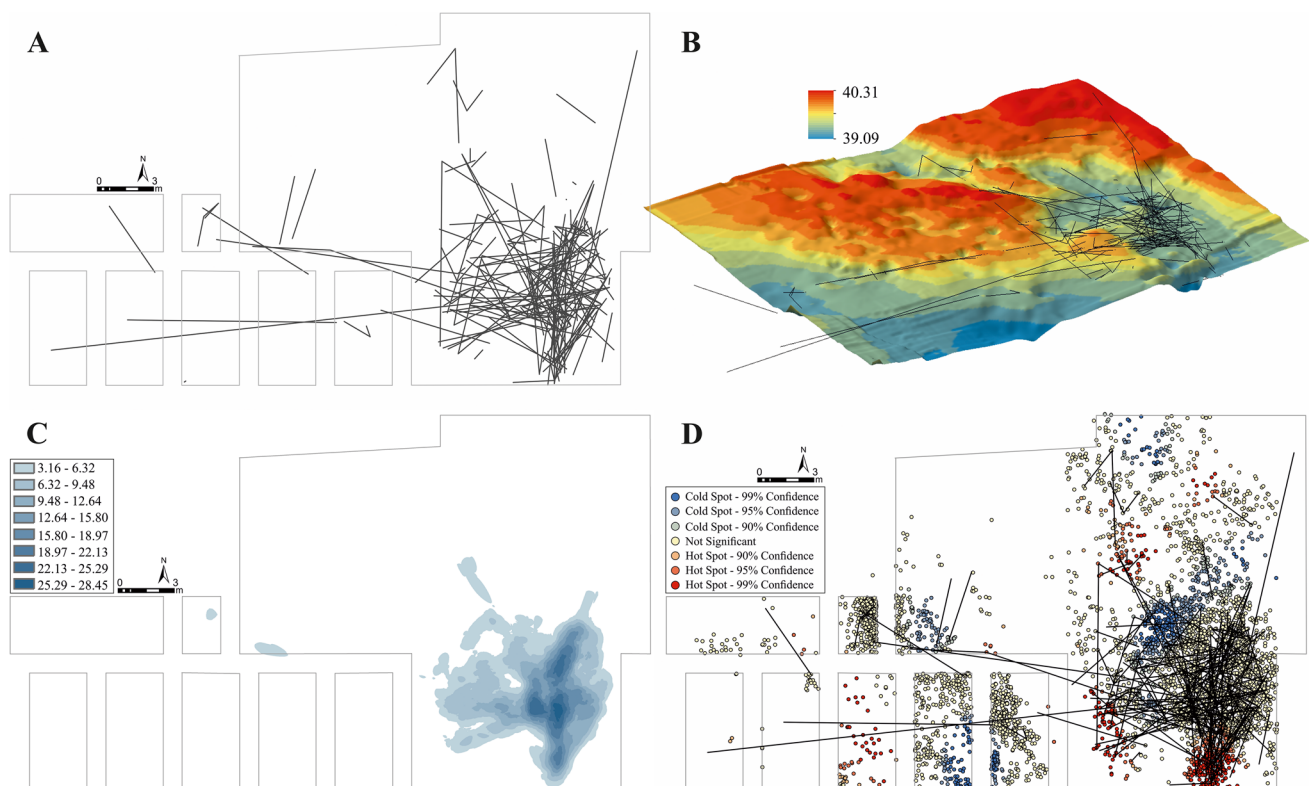


Fig. 12 **A** Map of refitting lines. **B** Distribution of refitting lines in the context of the palaeotopographic reconstruction of Unit 4u at Q1/B site. **C** KDE density map of refitting lines. **D** Getis-Ord G_i^* plan of lithic materials and refitting lines

Table 10 Statistical tests associated to the orientation patterns and eigenvalues with the 3D fabric results for the refitting lines of Q1/B site

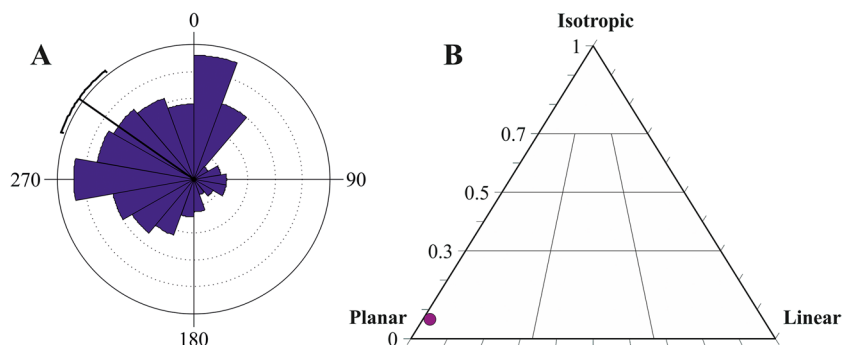
		Refitting lines	
Sample size	n	204	
Method		Azimuth	
Mean vector (°)	μ	305.37°	
Length of mean vector	r	0.344	
Concentration	k	0.732	
Circular Standard Deviation (°)	v	83.748°	
Rayleigh test	Z	24.086	
	p	3.46E-11	
Kuiper's test	V	3.901	
	p	< 0.01	

		Refitting lines	
Sample size	n	204	
E1	Azimuth	35.16	
	Plunge	0.72	
	Eigenvalue	99.224	
E2	Azimuth	305.13	
	Plunge	2.53	
	Eigenvalue	97.899	
E3	Azimuth	140.97	
	Plunge	87.37	
	Eigenvalue	6.877	
Parameters	K	0.005	
	C	2.669	
	I	0,069	
	E	0.013	
	F	0.070	
	C.L	>99%	

influence of the ups and downs of the fluctuations of the water level caused by seasonal moments. The lithic materials are, in general, more clustered than bones, something that can be noticed in the identified clusters, especially in the case of the coldspot cluster (Fig. 6). In the case of lithics, the MD hot and coldspot clusters partially coincide with the cluster NML and the limits marked by KDE. However, the rest of the clusters located at the west are on the margins of zones of maximum concentration delimited by KDE and Jenks (except the smaller cluster at the south). In this case, it seems that the accumulation patterns highlighted by KDE and Jenks are not correlated with the dynamics of accumulation according to the MD—beyond its coincidence because it is the larger accumulation area and the coincidence likelihood is high. In the case of bones, although the clusters are more dispersed, they coincide with the limits marked by KDE and Jenks, both in the main accumulation and the western cluster. This distribution could correspond to the

fact that bones may have been transported more easily, due to their lower density, and they floated far away generating this more dispersed distribution for this type of material. This distribution of clusters, together with the differences in orientation patterns between zones, may suggest the direction of the flow and the dispersion dynamics that affected the distribution of the materials. Additionally, and considering that in some cases there are clusters that remain on the edge of the basin, it is possible that fluctuations in the water level sorted the materials in these margins. This indicates movements that had been mainly produced within the pond, probably determined by the cliff located at the north and the coastline, both running E-W and not far from the location of the site. In addition, the results obtained for the archaeostratigraphic analysis show that the materials are more densely concentrated at the base of Unit 4u, while those at the top seem to be more dispersed (Fig. 13). This could indicate that the materials may have been concentrated by the

Fig. 13 **A** Circular histogram of the orientation patterns and **B** Benn's fabric diagram of refitting lines



processes that followed the initial erosion event, but at lower energy. This would help to explain the orientation patterns and the concentration of materials we find in the basins, and the differences that we observe between some parts.

The analysis of the orientation patterns of the refitting lines points to a movement mainly constrained to the basins. The fact that most of the distances are between 1 and 2 m could indicate that there were some displacements, and we can even infer some dynamics were as a result of the human activities performed at the site. However, the orientation results indicate a clear homogeneous pattern: more than 63% of the refitting lines are longer than 2 m (Table 8), which is too long to consider that they have not been affected by postdepositional processes. The refitting lines are recurrent in the central zone of the main basin, where hot and cold clusters have not been identified. This would indicate that, although this area has a higher density of refitting lines, and presumably more movement of pieces, there is not a sorting of materials by size (length). Indeed, we do not find a lack of pieces, but rather a concentration of materials of different

sizes. Apart from this, it is important to remark that there is also a greater recurrence of refitting lines joining within the main hotspot cluster (HL1), which could indicate an area of activity. In the rest of the assemblage, the recurrence of refitting lines is observed in those zones where clustering patterns according to MD were not detected, so it is possible that this recurrence could be because there is a greater exploitation of larger pieces. In this way, this part of the site could correspond to a central point where the main activities of knapping could have taken place, and from which other activities could have been performed in other parts of the site. This dynamic in the movement of pieces can be appreciated through the refitting lines and could be like those detected in the GTP17 site (Pope et al. 2020). However, this could also be because of the methodology used to conjoin the pieces that form the refits. The pieces contained in the main cluster are larger and hence much easier to refit. It is also important to consider the combination of information provided by the refits and archaeostratigraphy when they are projected together. The projection of refitting lines within

Fig. 14 Plan and projection of the archaeostratigraphic profiles delimited for the Boxgrove Q1/B site

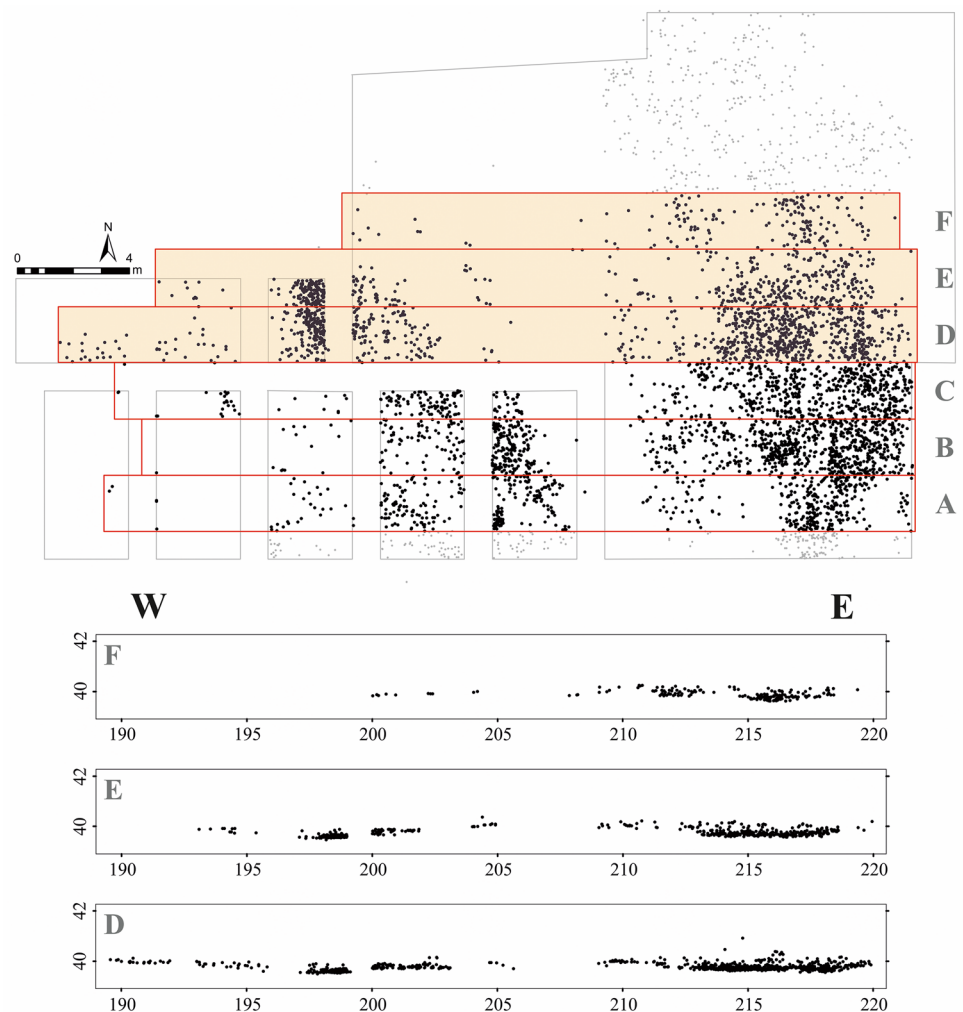
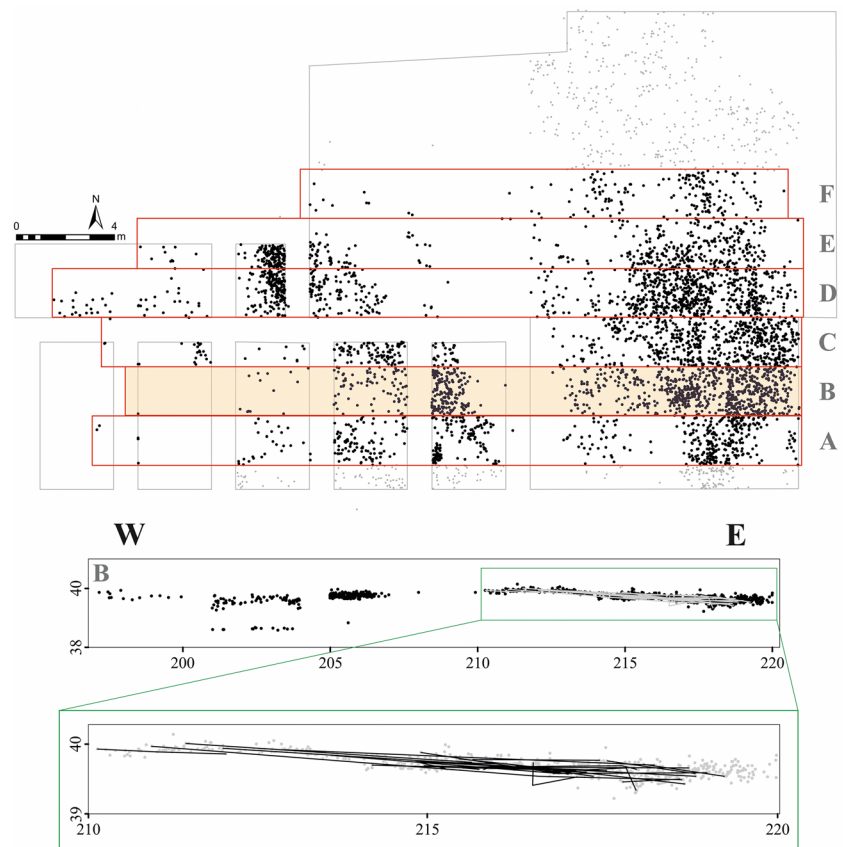


Fig. 15 Projection of refitting lines within the archaeostratigraphic profile B



the archaeostratigraphic profiles provides relevant information about the degree of preservation of the archaeological levels. Figure 15 shows many refitting lines concentrated in a single archaeostratigraphic profile, most of them showing a planar fabric (as also indicated by the 3D-fabric analysis for refits), and only a couple of lines crossing almost the vertical way of the profile. This evidence seems to support what the rest of the analyses also pointed out: that the deposit has been affected by some natural post-depositional processes but that they have been of a grade so low that they have hardly affected the materials.

The results obtained from the 3D fabric patterns for refit lines indicate a more planar result than when compared to individual bones and lithics. In this case, it is necessary to highlight that the refitting lines are being calculated, not just isolated pieces. The pattern obtained for the lithic pieces themselves shows movement consistent with water flow and influence by the slope of the underlying palaeotopography. Taken together, the analysis presented above is consistent with the impression given by the general disposition and conditions of the materials and initial taphonomic study (Pope 2002). As it has been pointed out before, both stone artefacts and faunal specimens are fresh and unabraded but are neither clustered nor articulated in a way that suggests

a pristine and undisturbed site. However, if the assemblage had been strongly affected by post-depositional processes, the position of the materials had been largely altered, and we would find refitting lines less concentrated and not constrained into specific zones (that is if refits were found). Our assessment of low-energy fluvial processes is consistent with the presence of ostracods with united valves, one of the best indicators of such conditions (Holmes et al. 2010).

Spatial studies in Palaeolithic archaeology have turned out to be a very interesting way to address and understand the site formation processes, considering both natural and human factors. This type of study is not centred on just one sort of variable, but also considers that which is actually extracted by spatial analysis itself in order to obtain a deep knowledge of the site that goes beyond the mere description of accumulation areas. The Boxgrove Q1/B site has been a challenge when approaching this study, with a large database and a particular problem given the context and the evident presence and development of activities by human groups at the site. Other open-air sites of similar chronology show analogous characteristics, but not all of them have provided deep spatial studies until now.

The sites of Neumark-Nord 1 (NN1) and Kärlich-Seeufer in Germany, Castel di Guido in Italy or Gesher Benot Ya'aqov

and Revadim Quarry in Israel have a very similar context to Q1/B, with large and very interesting assemblages. In the case of NN1, elephant bones were found in lacustrine deposits (Mania 1990; Fisher 2010; Palombo, 2010), which evidenced successive episodes of rising and lowering of the lake level (Mania 2004). The remains were found in lakeside sediments, not far from the shore, resulting in an excellent environment for the preservation of assemblages (Palombo 2012). Something similar happens with Kärlich-Seeufer, where human activity took place in the vicinity of a small lake with prevailing oligotrophic conditions (Gaudzinski et al. 1996). In the case of Castel di Guido, geological and taphonomic studies suggest that the site is a palimpsest with several phases of frequentation by humans, with partial reworking and removal of the fine fraction by low-energy flow (Saccà 2012a, b; Boschian and Saccà, 2015). Although slightly older than Q1/B, the Middle Pleistocene open-air site of Gesher Benot Ya'aqov is located on the shores of the paleo-Lake Hula in the northern Jordan Valley (Dead Sea Rift) (Alperson-Afil et al. 2009) and the study of the spatial distribution of materials showed the presence of dense concentrations of materials throughout the area (Alperson-Afil et al. 2009). This site was interpreted as slow-accumulation palimpsests by both natural and human agents (Goren-Inbar et al. 1992), like the site of Revadim Quarry where the artefact-bearing horizons were formed by high and low-energy hydraulic action (Malinsky-Buller et al. 2011). The stratigraphic sequence of this site indicates contexts of channel beds (Levels III and IV) and flood plains (Levels I and II), with large lithic and bone assemblages, which have served to provide information about the formation of the site and the distinction of several occupation levels (palimpsests) (Malinsky-Buller et al. 2011).

All these sites are very good examples of open-air sites in similar contexts and with comparable problems like the ones we find in Q1/B. However, most of them focus primarily on the identification and description of accumulation areas. By contrast, the review and application of new analysis methods and techniques at sites like Neumark-Nord 2 (García-Moreno et al. 2016) or the traditional sites of Schöningen (Böhner et al. 2015; García-Moreno et al. 2021) and Ambrona (Sánchez-Romero et al. 2016) have demonstrated the importance of spatial analysis to understand the site formation processes. In Spain, the localities of Venta Micena 4 and Barranco León, although older than Boxgrove, are examples where spatial analyses and landscape reconstruction were performed to infer the formation and accumulation of materials in the deposits of both localities (Titton et al. 2021; Luzón et al. 2021). Thus, it is possible to unravel the degree of influence and impact of natural factors on archaeological assemblages, the palaeotopography, context and, above all, human activity and intra-site dynamics resulting from the activities performed on the site and surroundings that have remained to the present day.

Identifying and locating the principal areas where the main behavioural activities took place is difficult, since a large area has clearly been affected by low-energy water flow. However, considering the results of the analyses relating to the distributional pattern of the materials and its relationship with the reconstructed context, it is possible that most of the activities could have been carried out at the southern area of the excavated area. Considering the model of occupation at the nearby site of GTP17 (Pope et al. 2020), it is likely that the main activities were located on the shore or in the immediate vicinity of the pond, where activities of knapping and tool configuration and carcass processing were combined. This proximity to the pond would have facilitated the identified movement of materials, due to water fluctuations that could have caused the reorganization and this pattern in the concentration of materials.

Conclusions

The spatial study of Boxgrove Unit 4u has made it possible to understand the succession of events involved in the formation of the archaeological record at this level. The study considers the spatial disposition of bones and lithic materials, their fabrics and the role of palaeotopography in their distribution, as well as the degree of influence of postdepositional factors. There are several statistically significant clusters, comprising both low and high values, according to the MD of bones and lithic materials. These clusters have been analysed both individually and as a whole, inferring causes that could have generated these accumulations in the context of the site. The spatial analysis has allowed us to put together all the elements and information relative to the spatial dispersion of materials, with the aim of unravelling the processes that took part in the accumulation of remains.

The results show that active fluvial processes worked during the formation of Unit 4u. Consequently, it is unthinkable that materials would maintain their original position, just as they were abandoned by human groups, without undergoing any kind of spatial rearrangement. However, while a pristine or minimally altered signature can be ruled out, the scale and nature of post-depositional movement determined in this study are consistent with artefacts being preserved within a primary depositional context. The identified low-energy post-depositional processes have not altered the condition or composition of the assemblages. The artefacts are still razor sharp and show no macroscopic signs of abrasion, the presence of very small debris remains and abundant refit factors consistent with the scale and nature of rearrangement identified in our spatial analysis.

We conclude that the Boxgrove Unit 4u assemblage can be taken to be a compositionally intact assemblage resulting from human activity around a freshwater body with variable

water levels during the period in which the archaeological signature was formed. A combination of movement due to the rising and falling water levels, most likely from springs to the north, could account for the scale of rearrangement determined by the analysis and is consistent with our current understanding of the locality. All seem to indicate low-energy activity that would have been delimited by the morphology of the pond, and therefore all activity is considered to have taken place within the limits of the pond, which may have varied in size with seasonal changes to the water table, and on its margins.

Furthermore, this study has revealed aspects of patterning which might relate more to behavioural factors rather than post-depositional transformations. These include localised concentrations that may have been primarily the product of focused human activity in the South-Eastern Basin (SEB) and apparent hiatuses in the deposition of materials which might relate to interruptions in human activity for unknown periods of time.

This study will allow us to apply similar levels of spatial analysis to the upper levels of the Q1/B site and understand the entire sequence, and its archaeological record, together, as part of a sedimentary system with unique affordances, such as freshwater, plant resources and game concentration, but also complex barriers to the simple analysis of the range of human behaviours giving rise to the record here. In the short term, it gives us greater confidence that the distinctive, biface-rich signature of the Q1/B assemblage is due to a higher proportion of bifaces being discarded at the site in comparison to other Boxgrove locales, rather than a product of post-depositional modification. It could also suggest that the two human lower incisors, found close together in the SEB basin, had not travelled far.

This study also contributes to the emerging discussion on the origin, distribution, culture and settlement of early Neanderthal populations in Europe. This work gives us the confidence that the Unit 4u horizon of Boxgrove Q1/B preserves the association of a bone and lithic assemblage, rich in bifaces, with teeth comparable to those of the Sima de los Huesos population. The teeth from both sites have been recently described as early Neanderthal (Lockey et al. 2022) and, while separated in time by over 50,000 years (Arnold et al. 2014) and in space by almost 1000 km, they both suggest the association of this population with a Late Acheulean culture.

Acknowledgements The excavations were directed by Mark Roberts and Simon Parfitt of the UCL Institute of Archaeology. The stone artefacts are curated at the British Museum, London, by Professor Nick Ashton who provided access for the study. We would like to thank Simon Parfitt for his comments, suggestions and fruitful discussions on the site. Thanks to Jo Mortimer for proofreading this manuscript.

Author contribution All authors contributed to the study conception and design. L. S-R. and M. P. wrote the first draft of the manuscript.

L. S-R. and A. B-C. performed the spatial analysis. All authors commented, reviewed and edited on previous versions of the manuscript. All authors read and approved the final manuscript.

Funding Open Access Funding provided by Universitat Autònoma de Barcelona. The Boxgrove Q1/B excavations ran from 1995 to 1996, and these works and post-excavation analysis were generously funded by Historic England.

Declarations

Consent to participate All authors consent to participate in this publication.

Competing interests The authors declare no competing interests.

Open Access This article is licensed under a Creative Commons Attribution 4.0 International License, which permits use, sharing, adaptation, distribution and reproduction in any medium or format, as long as you give appropriate credit to the original author(s) and the source, provide a link to the Creative Commons licence, and indicate if changes were made. The images or other third party material in this article are included in the article's Creative Commons licence, unless indicated otherwise in a credit line to the material. If material is not included in the article's Creative Commons licence and your intended use is not permitted by statutory regulation or exceeds the permitted use, you will need to obtain permission directly from the copyright holder. To view a copy of this licence, visit <http://creativecommons.org/licenses/by/4.0/>.

References

- Alpers-Afil N, Sharon G, Kislev M, Melamed Y, Zohar I, Ashkenazi S, Rabinovich R, Biton R, Werker E, Hartman G, Feibel C, Goren-Inbar N (2009) Spatial organization of hominin activities at Gesher Benot Ya'aqov, Israel. *Science* 326:1677–1680
- Anzidei AP, Bulgarelli GM, Catalano P, Cerilli E, Gallotti R, Lemorini C, Milli S, Palombo MR, Pantano W, Santucci E (2012) Ongoing research at the late Middle Pleistocene site of La Polledrara di Cecanibbio (central Italy), with emphasis on human–elephant relationships. *Quatern Int* 255:171–187
- Arnold LJ, Demuro M, Pares JM, Arsuaga JL, Aranburu A, Bermúdez de Castro JM, Carbonell E (2014) Luminescence dating and palaeomagnetic age constraint on hominins from Sima de los Huesos, Atapuerca, Spain. *J Hum Evol* 67:85–107
- Bargalló A, Gabucio MJ, Rivals F (2016) Puzzling out the palimpsest: testing an interdisciplinary study in level O of Abric Romani. *Quatern Int* 417:51–65
- Bargalló A, Gabucio MJ, Gómez de Soler B, Chacón MG, Vaquero M (2020) Rebuilding the daily scenario of Neanderthal settlement. *J Archaeol Sci Rep* 29:102139
- Behrensmeier AK (1988) Vertebrate preservation in fluvial channels. *Palaeogeogr Palaeoclimatol Palaeoecol* 63:183–199
- Benito-Calvo A, De la Torre I (2011) Analysis of orientation patterns in Olduvai Bed I assemblages using GIS techniques: implications for site formation processes. *J Hum Evol* 61(1):50–60
- Benito-Calvo A, Martínez-Moreno J, Jordá Pardo JF, De la Torre I, Mora Torcal R (2009) Sedimentological and archaeological fabrics in Palaeolithic levels of the South-Eastern Pyrenees: Cova Gran and Roca dels Bous sites (Lleida, Spain). *J Archaeol Sci* 36(11):2566–2577
- Benn DI (1994) Fabric shape and the interpretation of sedimentary data. *J Sediment Res* A64(4):910–915

- Benn DI, Ringrose TJ (2001) Random variation of fabric eigenvalues: implications for the use of axis fabric data to differentiate till facies. *Earth Surf Proc Land* 26(3):295–306
- Bertran P, Lenoble A (2002) Fabriques des niveaux archeologiques: methode et premier bilan des apports a l'etude taphonomique des sites paleolithiques. *Paleo* 14:13–28
- Bertran P, Texier JP (1995) Fabric analysis: application to Paleolithic sites. *J Archaeol Sci* 22(4):521–535
- Böhner U, Serangeli J, Richter P (2015) The Spear Horizon: first spatial analysis of the Schöningen site 13 II-4. *J Hum Evol* 89:202–213
- Boschian G, Saccà D (2010) Ambiguities in human and elephant interactions? Stories of bones, sand and water from Castel di Guido (Italy). *Quatern Int* 214:3–16
- Boschian G, Saccà D (2015) In the elephant, everything is good: carcass use and re-use at Castel di Guido (Italy). *Quatern Int* 361:288–296
- Bourguignon L, Sellami F, Deloze V, Sellier-segard N, Beyries S, Emery-barbier A (2002) L'habitat moustérien de "La Folie" (Poitiers, Vienne): Synthèse des premiers résultats. *PALEO*. <https://doi.org/10.4000/paleo.1389>
- Canals A, Vallverdú J, Carbonell E (2003) New archaeo-stratigraphic data for the TD6 level in relation to *Homo antecessor* (Lower Pleistocene) at the site of Atapuerca, north-central Spain. *Geoarchaeology* 18(5):481–504. <https://doi.org/10.1002/gea.10071>
- Chu W, Hosfield R (2020) Lithic artifact assemblage transport and microwear modification in a fluvial setting: a radio frequency identification tag experiment. *Geoarchaeology* 35:591–608. <https://doi.org/10.1002/gea.21788>
- Clark A (2017) From activity areas to occupational histories: new methods to document the formation of spatial structure in hunter-gatherer sites. *J Archaeol Method Theory* 24:1300–1325. <https://doi.org/10.1007/s10816-017-9313-7>
- Conard NJ, Serangeli J, Böhner U, Starkovich BM, Miller CE, Urban B, van Kolfschoten T (2015) Excavations at Schöningen and paradigm shifts in human evolution. *J Hum Evol* 89:1–17
- Cziesla E (1986) Über das Zusammenpassen von geschlagener Steinartefakte. *Archäologisches Korrespondenzblatt* 16:251–265
- Cziesla E (1990) On refitting stone artefacts. In: Cziesla E, Eickhoff N, Arts N, and Winter D (Eds.) *The Big Puzzle: International Symposium on Refitting Stone Artefacts*, Bonn, 9–44
- De la Torre I, Benito-Calvo A (2013) Application of GIS methods to retrieve orientation patterns from imagery: a case study from Beds I and II, Olduvai Gorge (Tanzania). *J Archaeol Sci* 40:1–12
- De la Torre I, Wehr K (2018) Site formation processes of the early Acheulean assemblage at EF-HR (Olduvai Gorge, Tanzania). *J Hum Evol* 120:298–328
- De la Torre I, Vanwezer N, Benito-Calvo A, Proffitt T, Mora R (2018) Spatial and orientation patterns of experimental stone tool refits. *Archaeol Anthropol Sci*. <https://doi.org/10.1007/s12520-018-0701-z>
- De la Torre I, Benito-Calvo A, Martín-Ramos C, McHenry LJ, Mora R, Njau JK, Pante MC, Stanistreet IG, Stollhofen H (2021) New excavations in the MNK Skull site, and the last appearance of the Oldowan and *Homo habilis* at Olduvai Gorge. *J Anthropol Archaeol* 61. <https://doi.org/10.1016/j.jaa.2020.101255>
- Falguères Ch, Bahain JJ, Pérez-González A, Mercier N, Santonja M, Dolo JM (2006) The Lower Acheulean site of Ambrona, Soria (Spain): ages derived from a combined ESR/U-series model. *J Archaeol Sci* 33:149–157
- Fisher K (2010) Die Waldelefanten von Neumark-Nord und Gröbern. In: Mania D (Ed.), *Ein interglaziales OkosystemdesmittelpaläolithischenMenschen. Veröffentlichungen des Landesamtes für Denkmalpflege und Archäologie Sanchsen-Anhalt, Landesmuseum für Vorgeschichte, Halle, Saale* 62, 361–373
- García-Medrano P, Ollé A, Ashton N, Roberts MB (2019) The mental template in handaxe manufacture: new insights into Acheulean lithic technological behavior at Boxgrove, Sussex, UK. *J Archaeol Method Theory* 26:396–422
- García-Moreno A, Smith GM, Kindler L, Pop E, Roebroeks W, Gaudzinski-Windheuser S, Klinkenberg V (2016) Evaluating the incidence of hydrological processes during site formation through orientation analysis. A case study of the Middle Palaeolithic Lake-land site of Neumark-Nord 2 (Germany). *Journal of Archaeological Science-Reports* 6:82–93
- García-Moreno A, Hutson JM, Villaluenga A, Turner E, Gaudzinski-Windheuser S (2021) A detailed analysis of the spatial distribution of Schöningen 13II-4 'Spear Horizon' faunal remains. *Journal of Human Evolution* 152. <https://doi.org/10.1016/j.jhevol.2020.102947>
- Gaudzinski S, Bittman F, Boenigk W, Frechen M, Van Kolfschoten T (1996) Palaeoecology and archaeology of the Kärlich-Seeufer open-air site (Middle Pleistocene) in the Central Rhineland, Germany. *Quatern Res* 46:319–334
- Getis A (1964) Temporal land-use pattern analysis with the use of Nearest Neighbor and Quadrat Methods. *Ann Assoc Am Geogr* 54(3):391–399
- Getis A, Ord JK (1992) The analysis of spatial association by use of distance statistics. *Geogr Anal* 24:3
- Goren-Inbar N, Belitzky S, Goren Y, Rabinovich R, Saragusti I (1992) Gesher Benot Ya'aqov – the "bar": an Acheulean assemblage. *Geoarchaeology* 7:27–40
- Goren-Inbar N, Lister A, Werker E, Chech M (1994) A butchered elephant skull and associated artifacts from the Acheulean site of Gesher Benot Ya'aqov, Israel. *Paléorient* 20:99–112
- Hillson SW, Parfitt SA, Bello SM, Roberts MB, Stringer CB (2010) Two hominin incisor teeth from the Middle Pleistocene site of Boxgrove, Sussex, England. *Journal of Human Evolution* 59(5):493–503
- Holmes JA, Atkinson T, Fiona Darbyshire DP, Horne DJ, Joordans J, Robert M (2010) Middle Pleistocene climate and hydrological environments at the Boxgrove hominin site (West Sussex, UK) from ostracod records. *Quaternary Science Review* 29(13–14):1515–1527
- Hutson JM, Villaluenga A, García-Moreno A, Turner E, Gaudzinski-Windheuser S (2020) A zooarchaeological and taphonomic perspective of hominin behaviour from the Schöningen 13II-4 "Spear Horizon." In: García-Moreno A, Hutson JM, Smith GM, Kindler L, Turner E, Villaluenga A, Gaudzinski-Windheuser S (eds) *Human Behavioural Adaptations to Interglacial Lakeshore Environments*. Verlag des Römisch-Germanischen Zentralmuseums, Mainz, pp 43–66
- Jenks GF (1967) The data model concept in statistical mapping. *Intern Yearbook Cartography* 7:186–190
- Lee J, Wong DWS (2000) *Statistical analysis with ArcView GIS*. Wiley
- Lenoble A, Bertran P (2004) Fabric of Palaeolithic levels: methods and implications for site formation processes. *J Archaeol Sci* 31(4):457–469
- Lockey AL, Rodríguez L, Martín-Francés L, Arsuaga JL, Bermúdez de Castro JM, Crété L, Martínón-Torres M, Parfitt S, Pope M, Stringer C (2022) Comparing the Boxgrove and Atapuerca (Sima de los Huesos) human fossils: do they represent distinct paleodemes? *J Hum Evol* 172:103253
- De Loecker D (2004) *Beyond the Site. The Saalian Archaeological Record at Maastricht-Belvédère (The Netherlands)*. *Analecta Praehistorica Leidensia*, 35–36, University of Leiden, Leiden
- Luzón C, Yravedra J, Courtenay LIA, Saarinen J, Blain H-A, DeMiguel D, Viranta S, Azanza B, Rodríguez-Alba JJ, Herranz-Rodrigo D, Serrano-Ramos A, Solano JA, Oms O, Agustí J, Fortelius M, Jiménez-Arenas JM (2021) Taphonomic and spatial analyses from the Early Pleistocene site of Venta Micena 4 (Orce, Guadix-Baza Basin, southern Spain). *Sci. Rep* 11:13977. <https://doi.org/10.1038/s41598-021-93261-1>
- Macphail RI, Goldberg P (2017) *Applied soils and micromorphology in archaeology*. Cambridge University Press

- Macphail RI (1996) The soil micromorphological reconstruction of the 500,000 year old hominid environment at Boxgrove, West Sussex, UK. In: Castelletti L, and Cremaschi M (Eds.) *Paleoecology. Colloquium VI. Micromorphology of deposits of anthropogenic origin. Colloquia of the XIII International Congress of Prehistoric and Protohistoric Sciences* 3:133–142
- Macphail RI (1999) Sediment micromorphology. In: Roberts, M. B. and Parfitt, S. (Eds.) *Boxgrove: A Middle Pleistocene hominid site at Earham Quarry, Boxgrove, West Sussex. English Heritage. Archaeological Report* 17
- Malinsky-Buller A, Hovers E, Marder O (2011) Making time: ‘Living floors’, ‘palimpsests’ and site formation processes – a perspective from the open-air Lower Palaeolithic site of Revadim Quarry, Israel. *J Anthropol Archaeol* 30:89–101. <https://doi.org/10.1016/j.jaa.2010.11.002>
- Mania D (1990) Stratigraphie, Ökologie und mittelpaläolithische Jagdbefunde des Interglazials von Neumark-Nord (Geiseltal), Veröff. Landesmuseum Vorgeschichte Halle 43:9–130
- Mania D (2004) In den Jagdgründen des Menschen vor 200.000 Jahren im Geiseltal. In Meller H (Ed.). *Kataloge zur Dauerausstellung im Landesmuseum für Vorgeschichte Halle “Paläolithikum und Mesolithikum”* 1:122–149
- Marder O, Malinsky-Buller A, Shahack-Gross R, Ackermann O, Ayalon A, Bar-Matthews M, Goldsmith Y, Inbar M, Rabinovich R, Hovers E (2010) Archaeological horizons and fluvial processes at the Lower Palaeolithic open-air site of Revadim (Israel). *J Hum Evol* 60(4):508–522. <https://doi.org/10.1016/j.jhevol.2010.01.007>
- McPherron SP (2018) Additional statistical and graphical methods for analyzing site formation processes using artifact orientations. *PLoS ONE* 13(1). <https://doi.org/10.1371/journal.pone.0190195>
- Mora Torcal R, Roy Sunyer M, Martínez-Moreno J, Benito-Calvo A, Samper Carro S (2020) Inside the palimpsest: identifying short occupations in the 497D level of Cova Gran (Iberia). In: Cascabeira J., Picin A. (Eds) *Short-Term Occupations in Paleolithic Archaeology. Interdisciplinary Contributions to Archaeology.* Springer
- Moran PAP (1950) Notes on continuous stochastic phenomena. *Biometrika* 37(1–2):17–23
- Oliver MA (1990) Kriging: a method of interpolation for geographical information systems. *Int. J. Geogr. Inf* 4(4):313–332
- Palombo MR (2010) The stylohyoideum of European palaeoloxodonts. *Quaternaire* 3 (Hors-série) 43–44
- Palombo MR (2012) Intra-specific variation of stylohyoid bones in Palaeoloxodon: a case study of Neumark-Nord 1 (Geiseltal, Sachsen-Anhalt, Germany) straight-tusked elephants. *Quatern Int* 276–277:77–92
- Pérez-González A, Santonja M, Benito A (2005) Secuencias litoestratigráficas del Pleistoceno medio del yacimiento de Ambrona. In Santonja M, and Pérez-González A (Ed.). *Los yacimientos paleolíticos de Ambrona y Torralba (Soria). Un siglo de investigaciones arqueológicas.* Zona Arqueológica 5:176–188
- Pope M, Roberts M, Maxted A, Jones P (2009) The Valdoe: archaeology of a locality within the Boxgrove palaeolandscape, West Sussex. In *Proceedings of the Prehistoric Society* (Vol. 75, pp 239–263). Cambridge University Press
- Pope M, Parfitt S, Roberts M (2020) The Horse Butchery Site: a high resolution record of Lower Palaeolithic hominin behaviour at Boxgrove, UK. *SpoilHeap Monograph* 23
- Pope M (2001) New investigations at Slindon Bottom Palaeolithic site, West Sussex: an interim report. *Lithics: The Journal of the Lithic Studies Society* 22
- Pope M (2002) The significance of biface-rich assemblages: an examination of behavioural controls on lithic assemblage formation in the Lower Palaeolithic (Doctoral dissertation, University of Southampton)
- Preece RC, Parfitt SA (2012) The Early and early Middle Pleistocene context of human occupation and lowland glaciation in Britain and northern Europe. *Quatern Int* 271:6–28. <https://doi.org/10.1016/j.quaint.2012.04.018>
- Radmilli AM, Boschian G (1996) Gli scavi a Castel di Guido, il più antico giacimento di cacciatori del Paleolitico inferiore nell’Agro Romano. Istituto Italiano di Preistoria e Protostoria, Firenze
- Ringrose TJ, Benn DI (1997) Confidence regions for fabric shape diagrams. *J Struct Geol* 19(12):1527–1536
- Ripley BD (1976) The second-order analysis of stationary point processes. *J Appl Probab* 13(2):255–266
- Roberts MB, Parfitt SA (1999) *Boxgrove: a Middle Pleistocene hominid site at Earham Quarry, Boxgrove, West Sussex. English Heritage, London*
- Roberts MB, Stringer CB, Parfitt SA (1994) A hominid tibia from Middle Pleistocene sediments at Boxgrove. *UK Nature* 369(6478):311–313
- Roberts MB, Pope MI (2009) The archaeological and sedimentary records from Boxgrove and Slindon. In RM Briant, MR Bates, RT, Hosfield and FF Wenban-Smith (Eds.), *The Quaternary of the Solent Basin and West Sussex raised beaches* (pp. 96–122). London: Quaternary Research Association Field Guide
- Roberts M, Pope M (2018) The Boxgrove wider area project. Mapping the early Middle Pleistocene deposits of the Slindon Formation across the Coastal Plain of West Sussex and eastern Hampshire. *Spoilheap Monograph* 15. Suffolk: Laveham Press
- Roberts MB, Bates MR, Bergman C, Currant AP, Haynes JR, Macphail R, McConnell A, Scaife R, Unger-Hamilton R, Whatley RC (1986) Excavation of the Lower Palaeolithic site at Amey’s Earham pit, Boxgrove, West Sussex: a preliminary report. In *Proceedings of the Prehistoric Society* 52(1):215–245. Cambridge University Press
- Romagnoli F, Vaquero M (2019) The challenges of applying refitting analysis in the Palaeolithic archaeology of the twenty-first century: an actualized overview and future perspectives. *Archaeol Anthropol Sci* 11:4387–4396
- Roy Sunyer M, Roda Gilabert X, Benito-Calvo A, Martínez-Moreno J, Mora Torcal R (2014) Verificando la integridad del registro arqueológico: Análisis de fábricas en las unidades arqueológicas del paleolítico medio/superior de la Cova Gran (Santa Linya, Lleida). *Treballs D’arqueologia* 20:55–77
- Saccà D (2012a) L’industria ossea di Castel di Guido (Roma) analisi tafonomica di bifacciali e strumenti poco elaborati. *Rivista di Scienze Preistoriche* LXII, 13–32
- Saccà D (2012b) Taphonomy of Palaeoloxodon antiquus at Castel di Guido (Rome, Italy): Proboscidean carcass exploitation in the Lower Palaeolithic. *Quaternary International* 276–277:27–41
- Sánchez-Romero L, Benito-Calvo A, Pérez-González A, Santonja M (2016) Assessment of accumulation processes at the Middle Pleistocene site of Ambrona (Soria, Spain). Density and orientation patterns in spatial datasets derived from excavations conducted from the 1960s to the Present. *PLoS One* 11(12):e0167595. <https://doi.org/10.1371/journal.pone.0167595>
- Sánchez-Romero L, Canals A, Pérez-González A, Márquez B, Mosquera M, Karampaglidis T, Arsuaga JL, Baquedano E (2017) Breaking the palimpsest: an approach to the cultural sequence of Neanderthal occupation at the Navalmafflo rockshelter, Pinilla del Valle (Spain). *Trab Prehist* 74(2):225–237
- Sánchez-Romero L (2019) Desarrollo y aplicación metodológica para el análisis espacial de yacimientos paleolíticos al aire libre y en cueva. PhD Dissertation. University of Burgos
- Sánchez-Romero L, Benito-Calvo A, Marín-Arroyo AB, Agudo L, Karampaglidis T, Rios-Garaizar J (2020) New insights for understanding spatial patterning and formation processes of the Neanderthal occupation in the Amalda I cave (Gipuzkoa, Spain). *Sci Rep* 10:8733. <https://doi.org/10.1038/s41598-020-65364-8>

- Sánchez-Romero L, Benito-Calvo A, Rios-Garaizar J (2021) Defining and characterising clusters in Palaeolithic sites: a review of methods and constraints. *J Archaeol Method Theory*. <https://doi.org/10.1007/s10816-021-09524-8>
- Sánchez-Romero L, Benito-Calvo A, San Emeterio A, Ortega I, Rios-Garaizar J (2022) Unraveling Châtelperronian high-density accumulations: the open-air site of Aranbaltza II (Bizkaia, Spain). *Archaeol Anthropol Sci* 14:77. <https://doi.org/10.1007/s12520-022-01541-2>
- Santucci E, Marano F, Cerilli E, Fiore I, Lemorini C, Palombo MR, Anzidei AP, Bulgarelli GM (2016) *Palaeoloxodon* exploitation at the Middle Pleistocene site of La Polledrara di Cecanibbio (Rome, Italy). *Quaternary International* 406(B):169–182
- Schick KD (1986) Stone age sites in the making: experiments in the formation and Transformation of archaeological occurrences. *British Archaeological Reports (BAR) International Series* 319. Oxford
- Serangeli J, Böhner U, van Kolfschoten, T, Conard NJ (2015) Overview and new results from large-scale excavations in Schöningen. *J Hum Evol* 89:27–45
- Siabato W, Guzmán-Manrique J (2019) La autocorrelación espacial y el desarrollo de la geografía cuantitativa. *Cuadernos de geografía. Revista colombiana de Geografía*, 28(1), 1–22. <https://doi.org/10.15446/rcdg.v28n1.76919>
- Silverman, (1986) Estimación de densidad para las estadísticas y el análisis de datos. Chapman and Hall, New York
- Sneed ED, Folk RL (1958) Pebbles in the lower Colorado River, Texas. A study in particle mophogenesis. *J Geol* 66(2):114–150
- Spagnolo V, Marciani G, Aureli D, Martini I, Boscato P, Boschin F, Ronchitelli A (2020) Climbing the time to see Neanderthal behaviour's continuity and discontinuity: SU 11 of the Oscurusciuto Rockshelter (Ginosa, Southern Italy). *Archaeol Anthropol Sci* 12:54
- Stein JK, Deo JN (2003) Big sites-short time: accumulation rates in archaeological sites. *J Archaeol Sci* 30:297–316
- Stout D, Apel J, Commander J, Roberts M (2014) Late Acheulean technology and cognition at Boxgrove, UK. *J Archaeol Sci* 41:576–590
- Stringer CB, Trinkaus E, Roberts MB, Parfitt SA, Macphail RI (1998) The Middle Pleistocene human tibia from Boxgrove. *J Hum Evol* 34(5):509–547
- Thieme H (1997) Lower Palaeolithic hunting spears from Germany. *Nature* 385:807–810
- Titton S, Oms O, Barsky D, Bargalló A, Serrano-Ramos A, García-Solano J, Sánchez-Bandera Ch, Yravedra J, Blain H-A, Toro-Moyano I, Jiménez Arenas JM, Sala-Ramos R (2021) Oldowan Stone knapping and percussive activities on a raw material reservoir deposit 1.4 million years ago at Barranco León (Orce, Spain). *Archaeol Anthropol Sci* 13:108. <https://doi.org/10.1007/s12520-021-01353-w>
- Wenban-Smith FF (1989) The use of canonical variates for determination of biface manufacturing technology at Boxgrove Lower Paleolithic site and the behavioural implications of this technology. *J Archaeol Sci* 16(1):17–26
- Whittaker JE, Parfitt SA (2017) The palaeoenvironment of the important Middle Pleistocene hominin site at Boxgrove (West Sussex, UK) as delineated by foraminifera and ostracods. In Williams M, Boomer TH, and Wilkinson IP (Eds.): *The archaeological and forensic applications of microfossils: a deeper understanding of human history*. The Geological Society of London 7. <https://doi.org/10.1144/TMS7.2>
- Woodcock NH (1977) Specification of fabric shapes using an eigenvalue method. *Geol Soc Am Bull* 88:1231–1236

Publisher's note Springer Nature remains neutral with regard to jurisdictional claims in published maps and institutional affiliations.